Identification of a Non-Canonical Ciliate Nuclear Genetic Code Where UAA and UAG Code for Different Amino Acids

Authors:

Jamie McGowan[1], Estelle S. Kilias[2], Elisabet Alacid[2], James Lipscombe[1], Benjamin H. Jenkins[2], Karim Gharbi[1], Gemy G. Kaithakottil[1], Iain C. Macaulay[1], Seanna McTaggart[1], Sally D. Warring[1], Thomas A. Richards[2], Neil Hall[1,3], David Swarbreck[1]

Affiliations:

[1] Earlham Institute, Norwich Research Park, Norwich, NR4 7UZ, UK

[2] Department of Biology, University of Oxford, Oxford, OX1 3SZ, UK

[3] School of Biological Sciences, University of East Anglia, Norwich, UK

Correspondence:

Thomas.Richards@biology.ox.ac.uk, Neil.Hall@earlham.ac.uk,
David.Swarbreck@earlham.ac.uk

Keywords: Genetic code, stop codon reassignment, Ciliophora, Oligohymenophorea, suppressor tRNA, phylogenomics

Abstract

The genetic code is one of the most highly conserved features across life. Only a few lineages have deviated from the “universal” genetic code. Amongst the few variants of the genetic code reported to date, the codons UAA and UAG virtually always have the same translation, suggesting that their evolution is coupled. Here, we report the genome and transcriptome sequencing of a novel ciliate, belonging to the Oligohymenophorea class, where the translation of the UAA and UAG stop codons have changed to specify different amino acids. Genomic and transcriptomic analyses revealed that UAA has been reassigned to encode lysine, while UAG has been reassigned to encode glutamic acid. We identified multiple suppressor tRNA genes with anticodons complementary to the reassigned codons. We show that the retained UGA stop codon is enriched in the 3’UTR immediately downstream of the coding region of genes, suggesting that there is functional drive to maintain tandem stop codons. Using a phylogenomics approach, we reconstructed the ciliate phylogeny and mapped genetic code changes, highlighting the remarkable number of independent genetic code changes within the Ciliophora group of protists. According to our knowledge, this is the first report of a genetic code variant where UAA and UAG encode different amino acids.

Introduction

The genetic code is one of the most conserved features across life, emerging before the last universal common ancestor [1]. Virtually all organisms use the canonical genetic code which has three stop codons (UAA, UAG, and UGA) and 61 sense codons that specify one of 20 amino acids, including a translation start codon (AUG). Variants of the genetic code, while rare, have been reported in several lineages of bacteria, viruses, and eukaryotic organellar and nuclear genomes [2,3]. Ciliate nuclear genomes are a particular hotspot for genetic code variation. The phylum Ciliophora is a large group of single-celled eukaryotes (protists) that diverged from other Alveolates more than one billion years ago [4]. Ciliates are highly unusual in that they exhibit nuclear dimorphism whereby each cell has two types of nuclei, the germline micronucleus (MIC) and the somatic macronucleus (MAC), each of which contains its own distinct genome structure and function [5]. The MIC genome functions as the germline genome and is exchanged during sexual reproduction. MIC genomes are typically diploid and are transcriptionally inactive during vegetative growth. The MIC genome undergoes rearrangement and excision of micronucleus-limited sequences to serve as a template to generate the transcriptionally active MAC genome [6]. MAC genomes typically contain short, fragmented, gene-dense chromosomes that are present at high ploidy levels (up to tens of thousands of copies) [7].

Known genetic code changes in ciliates involve reassignment of one or more stop codons to specify for amino acids. Most reported ciliate genetic code changes involve reassignment of both the UAA and UAG codons to specify glutamine as in *Tetrahymena*, *Paramecium*, and *Oxytricha* [8], or glutamic acid in *Campanella umbellaria* and *Carchesium polypinum* or tyrosine in *Mesodinium* species [9]. Other known modifications include reassignment of the UGA stop codon to specify tryptophan in *Blepharisma* [8], or cysteine in *Euplotes* [10]. The most extreme example of genetic code remodelling is found in

Condylostoma magnum where all three UAA, UAG, and UGA stop codons have been reassigned and can specify either an amino acid (glutamine for UAA and UAG, and tryptophan for UGA) or signal translation termination depending on their proximity to the mRNA 3’ end [9,11]. Not all ciliates use non-canonical genetic codes. For example, *Fabrea salina*, *Litonotus pictus*, and *Stentor coeruleus* use the canonical genetic code [9,12].

Changing the meaning of codons from stop to sense requires modifications to the translational apparatus. In eukaryotes, the eukaryotic release factor 1 (eRF1) protein recognises the three standard stop codons in mRNA and triggers translation termination. Studies have shown that mutations in the N-terminus of eRF1 can alter stop codon specificity [8,13–15]. eRF1 specificity to recognise only the UGA codon has evolved independently via different molecular mechanisms at least twice in ciliates with reassigned UAA and UAG codons [14]. Acquisition of tRNA genes with anticodons that recognise canonical stop codons (suppressor tRNAs), via mutations, base modifications or RNA editing enables translation of canonical stop codons into amino acids [16,17].

Tandem stop codons are additional stop codons located in the 3’-UTR within a few positions downstream of a gene in the same reading-frame [18]. They are thought to act as “back-up” stop codons in the event of readthrough, minimising the extent of erroneous protein elongation. For example, in yeast there is a statistical excess of stop codons in the third in-frame codon position downstream of genes with a UAA stop codon [18]. Tandem stop codons have been shown to be overrepresented in ciliates that only use UGA as a stop codon, compared to eukaryotes that use the canonical genetic code [19]. The level of overrepresentation is greater in highly expressed genes [20]. Tandem stop codons are thought to be particularly important in ciliates where, following stop codon reassignment, readthrough events might occur at a higher frequency due to mutations in eRF1 [20].

Several models have been proposed to describe genetic code changes. Under the “codon capture” model, a codon that is rarely used (e.g., due to GC content) is gradually eliminated from the genome followed by loss of the corresponding unused tRNA [21]. Due to random genetic drift the codon could reappear and be captured by a noncognate tRNA charged with a different amino acid, thus changing the genetic code. Such a process would be essentially neutral, not resulting in mistranslated protein products as the codon is eliminated from genes before the change in meaning occurs [17]. Alternatively, under the “ambiguous intermediate” model [22], reassignment of a codon takes place via an intermediate stage, where a codon is ambiguously translated via competing tRNAs charged with different amino acids, or in the context of stop codon reassignment, a suppressor tRNA competing with a release factor. This process would be driven by selection and result in the elimination of the cognate tRNA if the new meaning is advantageous. The “genome streamlining" model is more relevant to small genomes (e.g., organellar genomes or parasites) where there is pressure to minimise translational machinery [23]. More recently the “tRNA loss driven codon reassignment” mechanism was proposed to describe codon reassignments whereby tRNA loss, or alteration of release factor specificity, results in an unassigned codon that can be captured by another tRNA gene [24,25].

In virtually all genetic code changes reported to date, the codons UAA and UAG have the same meaning, i.e., they are either both used as canonical stop codons or are both reassigned to the same amino acid [25]. This suggests that evolutionary or mechanistic constraints couple the meaning of these two codons [26]. One such constraint is wobble binding of a suppressor tRNA gene with a UUA anticodon, where uracil in the first anticodon position can bind to either adenine or guanine in the third codon position of mRNA [27]. Thus, acquiring a suppressor tRNA gene with a UUA anticodon could potentially change the meaning of both the UAA and UAG codons. Wobble binding has been experimentally demonstrated in *Tetrahymena thermophila*, where tRNA-Sup(UUA) was shown to suppress both the UAA and UAG codons, whereas tRNA-Sup(CUA) suppressed only the UAG codon [16]. The first report of nuclear genetic code variants where UAA and UAG have different meanings were reported in transcriptomics analyses where a Rhizarian species (Rhizaria sp. exLh) was shown to use UAG to encode leucine and in a Fornicate (*Iotanema spirale*) where UAG has been reassigned to glutamine [26]. However, in both cases, the UAA codon was retained as a stop codon, thus avoiding the problem of genetic code ambiguity due to wobble binding.

Here, we report the discovery of a novel variant of the genetic code in a ciliate belonging to the Oligohymenophorea class, where the meaning of the UAA and UAG codons have changed to specify different amino acids. Using G&T-Seq [28], we performed parallel genome and transcriptome sequencing of small pools of ciliate cells. Combining genome and transcriptome sequencing data from multiple independently amplified samples enabled co-assembly of a highly complete macronuclear genome assembly and annotation. Genomic and transcriptomic analysis revealed that the UAA codon has been reassigned to specify lysine, while the meaning of the UAG codon has changed to specify glutamic acid. We identified multiple suppressor tRNA genes of both types in the genome, supporting the genetic code changes. We show that UGA codons are significantly enriched in the 3’-UTR of genes suggesting that there is selective pressure to maintain tandem stop codons, which may play a role in minimising erroneous protein elongation in the event of translational readthrough. To our knowledge, this is the first report of a genetic code variant where UAA and UAG specify different amino acids.

Results & Discussion

Genome Assembly of an Oligohymenophorean Ciliate

We isolated a novel ciliate species Oligohymenophorea sp. PL0344 from a freshwater pond at Oxford University Parks, Oxford, UK. Attempts to establish a stable long-term culture were unsuccessful so we applied low input single-cell based approaches to generate genomic and transcriptomic data. Small pools of cells (5 – 50 cells) were sorted into a microplate using fluorescence-activated cell sorting (FACS). Parallel genome and transcriptome sequencing was performed using G&T-Seq, which relies on whole genome amplification using multiple displacement amplification (MDA) and transcriptome analysis using a modified Smart-seq2 protocol [28].

A *de novo* genome assembly was generated by co-assembling reads from 10 samples (totalling approximately 6 Gb). Following manual curation and removal of contaminant sequences, the resulting macronuclear genome assembly was 69.7 Mb in length, contained in 3671 scaffolds with an N50 of 59.6 Kb (**Table 1**). Approximately 89% of the corresponding RNA-Seq reads mapped to the genome assembly, indicating high completeness. GC content of the genome is low at 30.6% (**Table 1**), which is similar to previously sequenced ciliate genomes [12]. The mitochondrial genome was also recovered which is a linear molecule 35,635 bp in length with GC content of 25.33% and capped with repeats. The mitochondrial genome contains the small subunit (SSU) and large subunit (LSU) ribosomal RNA (rRNA) genes, 5 tRNA genes, 19 known protein-coding genes, and 13 open reading frames.

The nuclear encoded SSU rRNA gene sequence is 99.81% identical to an environmental sequence (AY821923) of an unnamed ciliate in the GenBank database, isolated from Orsay, France [29]. Maximum-likelihood phylogenetic analysis of the SSU rRNA gene placed it within a clade containing four unnamed ciliate species (AY821923, HQ219368, LR025746, HQ219418) and *Cinetochilum margaritaceum* (MW405094) with

100% bootstrap support (**Supplementary Figure 1**). Thus, based on the SSU rRNA gene, *C. margaritaceum* is the closest related named species. The SSU rRNA gene of *C. margaritaceum* is 96.03% identical to that of Oligohymenophorea sp. PL0344. *C. margaritaceum* belongs to the Loxocephalida order (Class Oligohymenophorea; Subclass Scuticociliatia), which is considered a controversial order due to its non-monophyly [30,31]. Our phylogenetic analysis places *C. margaritaceum* as a divergent branch relative to other members of Loxocephalida (**Supplementary Figure 1**), which is congruent with previous analyses [30,31], suggesting taxonomic revision is required.

Oligohymenophorea sp. PL0344 Uses a Novel Genetic Code

Preliminary analysis of the genome sequence revealed that many coding regions contained in-frame UAA and UAG codons. Consistent with codon reassignments in other ciliate species, this suggested that the UAA and UAG stop codons have been reassigned to code for amino acids. Surprisingly however, the meanings of these codons do not match any known genetic code. An example gene (tubulin gamma chain protein), showing six in-frame UAA codons and six in-frame UAG codons, translated and aligned to orthologous protein sequences with representatives from across Eukaryota is displayed in **Figure 1**. Five in-frame UAA codons correspond to highly conserved columns in the alignment where lysine is the consensus amino acid (**Figure 1**). Four in-frame UAG codons correspond to highly conserved columns in the alignment where glutamic acid is the consensus amino acid, and another corresponds to a column with a mix of glutamic acid and aspartic acid (**Figure 1**).

We used two complementary tools to analyse the genetic code further. First, we used the “genetic_code_examiner” utility from the PhyloFisher package [32], which predicts the genetic code by comparing codon positions in query sequences to highly conserved (> 70% conservation) positions in amino acid alignments from a database of 240 orthologous protein sequences. PhyloFisher identified 58 genes with 87 in-frame UAA codons that correspond to highly conserved amino acid sites. Of these, 74 UAA codons (85%) correspond to highly conserved lysine residues (**Figure 2A**). The second most numerous match was to arginine, another positively charged amino acid, with 9 (10%) hits. PhyloFisher identified 46 genes with 63 in-frame UAG codons that correspond to highly conserved amino acid sites. Of these, 56 UAG codons (89%) correspond to highly conserved glutamic acid residues (**Figure 2B**). The second most numerous match was to aspartic acid, another negatively charged amino acid, with 4 (6%) of hits. Amongst the genes identified by PhyloFisher, 27 contained both in-frame UAA codons and an in-frame UAG codons.

We also analysed the genetic code using Codetta [33,34]. Codetta predicts the genetic code by aligning profile hidden Markov models (HMMs) from the Pfam database against a six-frame translation of the query genome assembly. The meaning of each codon is inferred based on emission probabilities of the aligned HMM columns. From the whole genome sequence, 14,633 UAA codons and 10,160 UAG codons had a Pfam position aligned. Based on these alignments, Codetta also predicted that the UAA codon is translated as lysine and UAG translated as glutamic acid, each with a log decoding probability of zero (**Figure 2C**).

Thus, these results indicate that Oligohymenophorea sp. PL0344 uses a novel genetic code where UAA is translated as lysine and UAG is translated as glutamic acid. This is the first time this genetic code variant has been reported. Furthermore, according to our knowledge, this is the first report of a genetic code variant where UAA and UAG have been reassigned to specify different amino acids. Genetic code variants were previously reported where UAG was reassigned to specify an amino acid (either leucine or glutamine) but UAA was retained as a stop codon in both cases [32]. This is significant as it suggests that the genetic code variant reported herein has overcome mechanistic constraints linking the translation of these two codons.

Suppressor tRNA Genes

tRNA genes were annotated using tRNAscan [35], resulting in the annotation of 320 tRNA genes, including 15 that are predicted to be pseudogenes. Amongst the annotated tRNA genes are 23 putative suppressor tRNA genes. These are tRNA genes with anticodons complementary to canonical stop codons (UAA, UAG, or UGA). The annotated suppressor tRNA genes include 12 tRNA-Sup(UUA) genes and 10 tRNA-Sup(CUA) genes. tRNAscan also predicted a single tRNA-Sup(UCA) gene, however this was low scoring and was not predicted by ARAGORN [36], an alternative tool to identify tRNA genes. tRNAscan also predicts the function of tRNAs. Many of the tRNAscan isotype predictions were consistent with the predicted genetic code (i.e., UAA = lysine and UAG = glutamic acid), however several putative tRNA genes had low-scoring or inconsistent isotype predictions. To better characterise the suppressor tRNA genes, we compared their sequences to the non-suppressor tRNA genes. Eight of the twelve predicted tRNA-Sup(UUA) genes were most similar to tRNA-Lys genes with UUU or CUU anticodons (68.49% to 80.95% identical) (**Supplementary Table 1**), consistent with the genetic code prediction that UAA has been reassigned to specify lysine. An example tRNA-Sup(UUA) predicted to function as a lysine tRNA is shown in **Figure 3A**. All ten tRNA-Sup(CUA) genes were most similar to tRNA-Glu genes with CUC or UUC anticodons (69.44% to 93.06% identical) (**Supplementary Table 1**), consistent with the genetic code prediction that UAG has been reassigned to specify glutamic acid. An example tRNA-Sup(CUA) predicted to function as a glutamic acid tRNA is shown in **Figure 3B**. Similarly, analysis using phylogenetic networks clusters most of the suppressor tRNA genes with tRNA genes of their predicted function (**Supplementary Figure 2**). We also identified a tRNA gene for selenocysteine, tRNA-SeC(UCA) **(Figure 3C)**, suggesting that the UGA codon is used both as a stop codon and to encode selenocysteine. Thus, all 64 codons can specify amino acids as has been reported in other ciliate genomes [37].

UAA and UAG codons differ only in the wobble position. According to wobble-binding rules, uracil in the first tRNA anticodon position ("wobble position") (**Figure 3A**) can bind to either adenine or guanine in the third codon position of mRNA [27], allowing tRNA with a UUA anticodon to recognise both UAA and UAG codons. It has been experimentally demonstrated that *T. thermophila* tRNA-Sup(UUA) can recognise both UAA and UAG codons [16]. It has been suggested that wobble binding is a possible explanation as to why UAA and UAG virtually always have the same meaning [9]. Considering that Oligohymenophorea sp. PL0344 has tRNA-Sup(UUA) genes for lysine and tRNA-Sup(CUA) genes for glutamic acid, this raises the question: are UAG codons ambiguously translated as both glutamic acid and lysine? If not, how has it overcome the mechanistic and evolutionary constraints that appear to couple the translation of these two codons? Presumably, if wobble binding allows tRNA-Sup(UUA) to recognise the UAG codon, it would be less efficient than tRNA-Sup(CUA) and outcompeted, possibly resulting in some degree of stochastically translated protein products with glutamic acid residues substituted by lysine at UAG codon positions. Attempts to establish a stable culture were unsuccessful, and while we can overcome this problem to generate a genome assembly using low-input sequencing methods designed for single-cell analysis, such low-input approaches are not available for proteomics. Without proteomics data, it is not possible to determine if UAG is ambiguously translated. Additionally, while the genomic and transcriptomic data provide strong evidence that lysine and glutamic acid are the major translation products of UAA and UAG codons, respectively, we cannot rule out the possibility that other amino acids are (mis)incorporated at these sites which could be detected using mass-spectrometry [38,39]. Furthermore, from suppressor tRNA gene sequences alone, it is not possible to determine if they incorporate modified nucleotides which could alter codon-anticodon binding specificity.

Genome Annotation and Codon Usage Analysis

Genome annotation incorporating RNA-Seq data and protein alignments from other ciliates resulted in the annotation of 22,048 transcripts from 20,141 gene models (**Table 1**). BUSCO analysis estimates that the genome annotation is highly complete with 94.7% of BUSCO genes recovered as complete, which compares favourably to other high quality ciliate genomes (**Supplementary Table 2**). The median intron size of 57 bp (**Table 1**) is similar to previously sequenced ciliate genomes, such as *Tetrahymena thermophila* and *Oxytricha trifallax* [7,37] but not as short as the extremely short introns (15 – 25 bp) found in *Stentor coeruleus* or *Paramecium tetraurelia* [12,40]. We defined a subset of genes as "highly expressed" based on the 10% of genes with the highest transcripts per million (TPM) values for comparison below. Codon usage is biased towards using codons with lower GC content. This bias is reduced in highly expressed genes which have higher GC content compared to all genes (38.51% versus 34.12%), similar to previous reports in *Paramecium* and *Tetrahymena* [37,41]. The reassigned codons are widely used across genes with 95.9% of genes containing both a UAA codon and a UAG codon. However, their usage is reduced in highly expressed genes (**Supplementary Table 3**). Reduced codon usage in highly expressed genes could indicate translational inefficiency, or that selective pressure to retain canonical lysine and glutamic acid codons is higher in highly expressed genes.

Very little is known about translation termination efficiency in ciliates. This is particularly interesting for ciliates that use only UGA as a stop codon, as UGA is known to be the least robust stop codon and the most prone to translational readthrough [42]. The sequence composition surrounding a stop codon influences the rate of stop codon readthrough. The nucleotide immediately downstream of a stop codon (+4 position) is particularly important, with several studies demonstrating that presence of a cytosine following UGA substantially increases the rate of readthrough [43–45]. Interestingly, examining the sequence composition surrounding stop codons in Oligohymenophorea sp. PL0344, cytosine appears to be avoided following the stop codon (**Supplementary Figure 3**). This is particularly noticeable in highly expressed genes (**Supplementary Figure 3**) where the proportion of genes with a cytosine following UGA is significantly reduced (chi-squared test, p-value = 7.3e-10). This trend has also been observed in *P. tetraurelia* and *T. thermophila* [41]. Tandem stop codons potentially play an important role as "back-up" stop codons, minimising the extent of protein elongation in the event of readthrough [18]. Here, we analysed tandem stop codons by counting UGA codons in the first 20 in-frame codon positions downstream of genes. Our results show that UGA codons are significantly overrepresented (chi-squared test, p-value < 0.05) in the first four in-frame codons downstream of genes (**Figure 4**). 12.3% of genes have at least one UGA codon within the first six in-frame codon positions downstream of genes, similar to the proportion reported for *T. thermophila* (11.5%) where UAA and UAG have also been reassigned to encode amino acids [19]. For comparison, the reassigned UAA and UAG codons are not overrepresented in this region. The frequency of UGA codons at these positions is greater for highly expressed genes whereby 13.6% of highly expressed genes have at least one UGA codon within the first six in-frame codon positions downstream of genes (**Figure 4**). These data add support that there is selective pressure for ciliates with reassigned UAA and UAG codons to maintain tandem UGA stop codons at the beginning of the 3'-UTR. It is tempting to speculate that these additional UGA stop codons play a role in minimising deleterious consequences of readthrough events.

Phylogenomics Analysis of Genetic Code Changes in the Ciliophora

We carried out phylogenomics analyses to map genetic code changes onto the ciliate phylogeny. A phylogenomic dataset consisting of genomic and transcriptomic data from 46 ciliate species and 9 outgroup species was constructed (**Supplementary Table 2**). Phylogenomic reconstruction was performed on a concatenated alignment of 89 single-copy BUSCO proteins (40,289 amino acid sites) using maximum-likelihood (IQ-TREE under LG+F+I+R7 model) and Bayesian (PhyloBayes-MPI under CAT-GTR model) approaches. We also conducted a partitioned analysis on the same dataset using IQ-TREE, with a partitioning scheme which merged the 89 proteins into 14 partitions. The three resulting phylogenies were largely in agreement with each other and with previously published analyses, with full or high support from all three methods at most branches (**Figure 5**). Oligohymenophorea sp. PL0344 was robustly placed within the Oligohymenophorea class in a clade containing Hymenostomatida and *Pseudocohnilembus persalinus* with full support from all three methods (**Figure 5**).

The position of *Paramecium* (order Peniculida) is unstable in our phylogenomic analyses. Both the LG+F+I+R7 and partitioned phylogeny group *Paramecium* as sister to the Peritrichia clade with 89% and 82% bootstrap support respectively (**Figure 5**). This is congruent with some previous phylogenomic analyses which recover Peniculida as sister to Peritrichia species [46–48]. However, the Bayesian phylogeny places *Paramecium* as sister to Hymenostomatida and Philasterida (**Supplementary Figure 4**). This grouping has been recovered in some previous phylogenomic analyses [49,50]. The correct placement of Peniculida is unclear based on the current datasets available. The *Paramecium* species included in our analysis have a high proportion of missing data (**Figure 5**). We anticipate that differences in topology may be influenced by varying levels of sensitivity to missing data in the models used. *Mesodinium rubrum* is another problematic taxon which is thought to be prone to long branch attraction (LBA) artefacts. Furthermore, existing *Mesodinium* transcriptomes are contaminated with sequences from their prey [51]. Some previous phylogenomic and phylogenetic analyses place it as an early branching ciliate [52,53], however these may have been influenced by contamination [51]. Here, we account for contamination by removing any sequences from the *M. rubrum* transcriptome with best BLAST hits outside of the Ciliophora (n = 3,574). Both the LG+F+I+R7 and partitioned phylogeny group *M. rubrum* with *Litonotus pictus,* another member of the Litostomatea class, with 85% and 93% bootstrap support respectively (**Figure 5**), while our Bayesian analysis places it as a deep branching ciliate branching before *Protocruzia* (**Supplementary Figure 4**). The grouping of *M. rubrum* with *L. pictus* agrees with a recent phylogenomics analysis of *Mesodinium* species that accounts for LBA and contamination [51].

Where genome or transcriptome assemblies were available, or raw sequencing reads deposited in public databases, we validated the known genetic codes using Codetta and PhyloFisher. All species had the expected genetic code except for *Plagiopyla frontata*. Codetta and PhyloFisher both predicted that UAA and UAG are translated as glutamine in *P. frontata*, which is not surprising given how many ciliate species use this genetic code (**Figure 5**). Interestingly however, both methods predict that UGA has also been reassigned to specify tryptophan in *P. frontata*. From the PhyloFisher dataset of 240 query proteins, 3 (1.25%) contain internal UGA codons that correspond to highly conserved tryptophan residues in other species **(Supplementary Figure 5).** This suggests that *P. frontata* may use UGA both as a stop codon and also rarely as a sense codon to specify tryptophan, similar to the *Condylostoma* genetic code (**Figure 5**) [9,11].

We mapped genetic code reassignments onto the ciliate phylogeny, highlighting the remarkable number of independent genetic code changes within the ciliates (**Figure 5**). Based on our phylogeny, and assuming a non-canonical genetic code doesn't revert to the canonical genetic code, the translation of UAR (UAA and UAG) codons to glutamine is the most common genetic code variant and has independently evolved at least five times. From our analysis, translation of UGA to tryptophan has independently evolved at least three times in ciliate nuclear genomes. However, it has recently been reported that Karyorelict ciliates (not included in this analysis) use a context-dependent genetic code similar to *Condylostoma*, where UAR has been reassigned to glutamine and UGA specifies either tryptophan or stop depending on context, indicating a fourth independent origin of UGA being translated as tryptophan and a sixth independent origin of UAR being translated to glutamine in ciliates [54]. The translation of UGA to cysteine in *Euplotes*, UAR to tyrosine in *Mesodinium* and UAR to glutamic acid in Peritrichia have all evolved once. The Oligohymenophorea sp. PL0344 genetic code appears to be a relatively recent phenomenon and is unique in that the two codons have different meanings. The Oligohymenophorea class contains at least three different genetic code variants, and no sampled species which have retained usage of UAA or UAG as a stop codon. Our phylogeny suggests that the stop codons UAA and UAG were reassigned to glutamine in the ancestor of Oligohymenophorea (**Figure 5**). These codons were then reassigned to glutamic acid in the Peritrichs, or to lysine (UAA) and glutamic acid (UAG) in Oligohymenophorea sp. PL0344.

It remains unclear why Ciliate genomes are such a hotspot for stop codon reassignments. Our study shows that even within the Oligohymenophorea class, which is relatively well sampled compared to other ciliate clades, there remain novel genetic code reassignments to be discovered. Further sequencing of under-sampled ciliate lineages and other microbial eukaryotes may reveal more variant genetic code changes and help to better understand the evolution and mechanisms of genetic code changes.

Materials and methods

Sampling, Ciliate isolation, Culturing, and Cell-sorting

Surface water was collected from a margin of an artificial freshwater pond at Oxford University Parks (51°45'51.0"N 1°15'04.5"W), Oxford (UK) by directly submerging a 1 litre autoclaved glass collection bottle. 200 mL of the water sample were concentrated using a 5 µm filter into a final volume of 20 mL. Oligohymenophorea sp. PL0344 was identified using an inverted microscope (Olympus CKX41) and single cells were isolated manually using a glass micropipette by transferring them into successive drops of 0.2 µm pre-filtered and autoclaved environmental source water. When cells were free of any other eukaryote, they were transferred into a 96 well-plate containing filtered and autoclaved environmental source water. In order to obtain a clonal culture, isolated cells were incubated during a week at 20^oC with a 12h:12h light:dark photo-cycle with a photon flux of 32 $\mu moles \cdot m^{-2} \cdot s^{-1}$. When ciliate cells divided and a dense culture was observed in the well, the mini-culture was scaled-up during a month by successively transferring the cells into larger volumes until a non-axenic but monoeukaryotic ciliate culture of 20 mL of volume was established. Pools of ciliate cells (5 – 50 cells) were then sorted into a 384-well plate containing 5 µL of autoclaved source water using FACS (BD FACSMelody™ Cell Sorter, BD Biosciences). 10 µL of RLT+ lysis buffer (Qiagen) was then added to each well and the plate was sealed and centrifuged (2000 x g, 4 ºC, 1 min) to remove bubbles and to ensure that the lysis buffer was at the bottom of each well. The sorted plate was stored at -80ºC until processed.

G&T-Seq, Library Preparation, and Sequencing

Using a magnetic separator, Dynabeads™ MyOne™ Streptavidin C1 (Invitrogen) beads were washed according to the manufacturer's guidance and then incubated with 2 × Binding &Wash buffer (10 mM Tris-HCl pH 7.5, 1 mM EDTA, 2 M NaCl) and Biotinylated Oligo-dT primer (IDT, 5’-/BiotinTEG/AAG CAG TGG TAT CAA CGC AGA GTA CTT TTT TTT TTT TTT TTT TTT TTT TTT TTT TVN-3’) at 100 µM for 30 minutes at room temperature on a rotator. The oligo-treated beads were washed four times in 1 × Binding &Wash buffer (5 mM Tris-HCl pH 7.5, 0.5 mM EDTA, 1 M NaCl) and then suspended in 1 × SuperScript II First Strand Buffer (Invitrogen) supplemented with SUPERase•In™ RNase Inhibitor (Invitrogen) to a final concentration of 1 U/µl. The lysate was thawed on ice. 10 µl of prepared oligo-dT beads was added to each well containing 12 µl cell lysate. The lysate plate was sealed and incubated on a ThermoMixer C (Eppendorf) at 21 °C for 20 minutes shaking at 1000 rpm. Using a Fluent 480 liquid handling robot (Tecan) and a Magnum FLX magnetic separator (Alpaqua), the lysate supernatant was transferred to a new plate and the beads were washed twice in a custom wash buffer (50 mM Tris-HCl pH 8.3, 75 mM KCl, 3 mM $MgCl_2$, 10 mM DTT, 0.5% Tween-20). The supernatant from the washes was added to the left-over cell lysate - containing the genomic DNA - which was stored at -20 °C overnight. The washed beads were suspended in a reverse transcription mastermix of 1 mM dNTPs, 0.01 M $MgCl_2$,1 × SuperScript II First Strand Buffer, 1 M Betaine, 5.4 M DTT, 1µM Template-Switching Oligo (5′-AAGCAGTGGTATCAACGCAGAGTACrGrG+G-3′, where “r” prefixes a ribonucleic acid base and “+” prefixes a locked nucleic acid base, Qiagen) then incubated using a ThermoMixer C with the following conditions: 42 °C for 2 minutes at 200 rpm, 42 °C for 60 minutes at 1500 rpm, 50 °C for 30 minutes at 1500 rpm, 60 °C for 10 minutes at 1500 rpm. The cDNA was amplified using HiFi Hotstart Ready Mix (KAPA) and IS Primers to a final concentration of 0.1 µM (IDT, 5’-AAG CAG TGG TAT CAA AGA GT-3’) with the following thermocycling conditions: 98 °C for 3 minutes, then 21 cycles of 98 °C for 15 seconds, 67 °C for 20 seconds, 72 °C for 6 minutes and finally 72 °C for 5 minutes. The cDNA was then purified using 0.8 × vols Ampure XP (Beckman Coulter) and 80% ethanol on the Fluent 480 liquid handling robot and eluted in 10 mM Tris-HCl. The remaining cell lysate was thawed and subjected to a 0.6 × vols Ampure XP clean-up with 80% ethanol. The bead-bound gDNA was isothermally amplified for 3 hours at 30 °C then 10 minutes at 65 °C using a miniaturised (1/5 vols) Repli-g Single-Cell assay (Qiagen). The amplified gDNA was cleaned up with 0.8 × vols Ampure XP and 80 % ethanol, then eluted in 10 mM Tris-HCl. The cDNA and gDNA were quantified by fluorescence (Quant iT HS-DNA, Invitrogen) on an Infinite Pro 200 plate reader (Tecan) then normalised to a final concentration of 0.2 ng/µl in 10 mM Tris-HCl. Dual-indexed sequencing libraries (Nextera XT, Illumina) were prepared using Mosquito and Dragonfly liquid handling instruments (SPT Labtech). The libraries were pooled and cleaned up using 0.8 × vols Ampure XP and 80% ethanol. The libraries were eluted in 10mM Tris-HCl and assessed using a Bioanalyzer HS DNA assay (Agilent), HS DNA Qubit assay (Invitrogen) and finally an Illumina Library Quantification Kit assay (KAPA). Sequencing was conducted on a NovaSeq 6000 with a 300 cycle Reagent kit v1.5 (Illumina) to produce 150 bp paired-end, dual-indexed reads.

Genome Assembly

Adapter and quality trimming were carried out using BBDuk (https://jgi.doe.gov/data-and-tools/bbtools). Reads which mapped to a database of common lab contaminants (human and mouse) were removed using BBMap. A co-assembly of genomic DNA reads from 10 samples was generated using SPAdes (v3.15.3) [55] with default settings except -k 21, 33, 55, 77 and single-cell mode (--sc) was enabled. The assembly was manually curated and contaminant contigs were removed using a combination of metagenomic binning with MetaBAT2 [56] based on tetra-nucleotide frequencies and taxonomic classification with CAT (v5.2) [57] and Tiara (v1.0.1) [58]. Independent genome assemblies were also generated for all 10 individual samples and average nucleotide identities were compared as a quality control step to confirm that they corresponded to the same species. Assembly statistics were calculated using Quast [59]. Genome completeness was assessed using BUSCO (v4.1.2) [60] with the Alveolata_obd10 dataset run in genome mode.

Genome Annotation

The genetic code was predicted using Codetta (v2.0) [33,34] and also using the “Genetic Code Examiner” utility from the PhyloFisher package, with the included database of 240 orthologs [32].

Gene models were annotated via the Robust and Extendable eukaryotic Annotation Toolkit (REAT, https://github.com/EI-CoreBioinformatics/reat) and Minos (https://github.com/EI-CoreBioinformatics/minos) using a workflow incorporating repeat identification, RNA-Seq mapping / assembly, alignment of protein sequences from related species and evidence guided gene prediction with AUGUSTUS [61].

A de novo repeat annotation was created using the RepeatModeller [62] v1.0.11 - RepeatMasker v4.07 [63] pipeline with defaults settings and the --gff output option enabled. To ensure high copy number ‘bonafide’ genes were excluded from repeat masking, the RepeatModeler library was hard masked using protein coding genes from 11 ciliate species (detailed below). The protein coding genes were first filtered to remove any genes with descriptions indicating "transposon" or "helicase". TransposonPSI (r08222010) http://transposonpsi.sourceforge.net was then run to remove any transposon hits by hard-masking them and using the filtered gene set to mask the RepeatModeler library. RepeatMasker v4.0.7 was run with the Repbase Alveolata library (RepBaseRepeatMaskerEdition-20170127.tar.gz) and additionally with the filtered RepeatModeler library. The interspersed repeats were combined and used as evidence in the gene build.

The REAT transcriptome workflow was run with RNA-Seq (total 77 million read pairs) from 28 samples. As transcriptome assembly is sensitive to depth of RNA-Seq coverage samples were combined into sets of 28, 10, 10 and 8 samples to ensure reasonable coverage but also allow alternative assemblies to be created. Illumina RNA-seq reads were mapped to the genome with HISAT2 v2.2.1 [64] and high-confidence splice junctions identified by Portcullis [65]. The aligned reads were assembled for each set of samples with StringTie2 v2.1.5 [66] and Scallop v0.10.5 [67]. From the combined set of RNA-Seq assemblies a filtered set of non-redundant gene-models were derived using Mikado [68]. The REAT homology workflow was used to generate gene models based on alignment of proteins from 11 ciliate species (**Supplementary Table 2**). These together with the transcriptome derived models were used to train the AUGUSTUS v3.4.0 gene predictor, with transcript and protein alignments plus repeat annotation provided as hints in evidence guided gene prediction using the REAT prediction workflow. Six alternative AUGUSTUS gene builds were generated using different evidence inputs or weightings for the protein, transcriptome and repeat annotation. The Minos pipeline was run to generate a consolidated set of gene models from the transcriptome, homology, and AUGUSTUS predictions. The pipeline utilises external metrics to assess how well supported each gene model is by available evidence, based on these and intrinsic characteristics of the gene models a final set of models is selected. For each gene model a confidence and biotype classification were determined based on the type and extent of supporting data.

Annotation completeness was assessed using BUSCO (v4.1.2) [60] with the Alveolata_obd10 dataset run in protein mode. tRNA genes were annotated using tRNAscan (v2.0.7) [35]. rRNA genes were annotated using barrnap (v0.9) (https://github.com/tseemann/barrnap).

Tandem Stop Codon Analysis

To investigate if UGA stop codons are enriched in the 3’-UTR of genes, codon usage of the first 20 in-frame codons downstream of each gene’s stop codon was calculated. Expected frequencies were determined by counting codons in all six reading frames in the 60 bp region downstream of each gene’s stop codon. We also carried out this analysis for highly expressed genes which we defined as the 10% of genes with the highest transcripts per million (TPM) values, calculated using Kallisto [69]. Statistical significance was assessed using the chi-squared test.

Phylogenetic Analysis of SSU rRNA Genes

Small subunit ribosomal RNA sequences from related species were retrieved from GenBank (**Supplementary Figure 1**). Sequences were aligned using MAFFT (v7.490) with the G-INS-I algorithm [70]. Maximum-likelihood phylogenetic analysis was performed using IQ-TREE (v2.2.0) [71] under the GTR+F+R5 model, which was the best fit model according to ModelFinder [72], with 100 non-parametric bootstrap replicates.

Phylogenetic Network Analysis of tRNA Genes

A multiple sequence alignment of tRNA genes was generated using MAFFT (v7.490) with the G-INS-I algorithm [70]. tRNA genes predicted to be pseudogenes, containing introns, or that were excessively truncated were excluded. A Neighbour-Net phylogenetic network was constructed using SplitsTree4 [73].

Phylogenomic Analyses

A phylogenomic dataset of 55 species was assembled including previously published ciliate genomes and transcriptomes with outgroup species from the Alveolata, retrieved from databases and published phylogenomics analyses [74,75] (**Supplementary Table 2**). *De novo* transcriptome assemblies were generated for two species – *Campanella umbellaria* and *Carchesium polypinum*. RNA-Seq reads were retrieved from the sequence read archive (SRR1768423 and SRR1768437) [46]. Transcriptome assemblies were generated using Trinity [76], redundancy was reduced using CD-HIT-EST [77] with an identity cut-off of 98% and protein coding transcripts were predicted using Transdecoder [78]. Coding sequences were translated into amino acids using the correct genetic code (UAR = E). The transcriptome assembly of *Mesodinium rubrum* is contaminated with sequences from its prey. We excluded any *M. rubrum* proteins with a best BLAST hit outside of the Ciliophora to account for this contamination which resulted in the removal of 3,574 (22%) proteins.

BUSCO analysis using the Alveolata_obd10 dataset identified 89 proteins that are present and single copy in at least 65% of species, i.e., at least 36 out of 55 species. Each BUSCO family was individually aligned using MAFFT (v7.490) [70] and then trimmed using trimAl (v1.4) with the "gappyout" parameter [79]. The trimmed alignments were concatenated together resulting in a supermatrix alignment of 40,289 amino acid sites. Maximum-likelihood phylogenetic reconstruction was performed using IQ-TREE (v2.2.0) [71] under the LG+F+I+R7 model, which was the best fitting model according to ModelFinder [72], and 100 non-parametric bootstrap replicates were used to assess branch support. We also conducted a partitioned analysis using IQ-TREE [80] with a partitioning scheme that merged the 89 proteins into 14 partitions with model selection performed by ModelFinder, with 100 non-parametric bootstrap replicates. Bayesian analyses were also performed on the supermatrix alignment using PhyloBayes-MPI (v1.8c) [81] under the CAT-GTR model. Constant sites (n = 3,299) were removed. Two independent Markov chain

Monte Carlo (MCMC) chains were run for approximately 12,000 generations. Convergence was assessed using bpcomp and tracecomp with a burn-in of 20%.

Acknowledgements

This work was funded by Wellcome though the Darwin Tree of Life Discretionary Award (218328) and supported by the Biotechnology and Biological Sciences Research Council (BBSRC), part of UK Research and Innovation, through the Core Capability Grant BB/CCG1720/1 at the Earlham Institute. Part of this work was delivered via the BBSRC National Capability in Genomics and Single Cell Analysis (BBS/E/T/000PR9816) at Earlham Institute by members of the Genomics Pipelines, Single-Cell and Core Bioinformatics Groups, the authors, note the specific contributions of Tom Barker, Vanda Knitlhoffer and Chris Watkins. Additional work was delivered via the BBSRC National Capability in e-Infrastructure (BBS/E/T/000PR9814) at the Earlham Institute by members of the e-Infrastructure group. The authors would like to acknowledge the Scientific Computing group, as well as support for the physical HPC infrastructure and data centre delivered via the NBI Research Computing group. TAR is supported by a Royal Society University Research Fellowship (URF/R/191005).

Data Availability

All sequencing data and the genome assembly of Oligohymenophorea sp. PL0344 have been deposited to the European Nucleotide Archive under the study accession PRJEB58266. Additional supporting data have been deposited on Zenodo (10.5281/zenodo.7944379).

Figure Legends

Figure 1: Genetic code change in Oligohymenophorea sp. PL0344. Example multiple sequence alignment of a tubulin gamma chain protein and orthologous sequences spanning Eukaryota. The alignment has been trimmed for visualisation purposes to remove poorly conserved regions and highlight internal UAA and UAG codons.

Figure 2: Genetic code prediction for Oligohymenophorea sp. PL0344. PhyloFisher genetic code prediction for the **(A)** UAA and **(B)** UAG codons using the PhyloFisher database of 240 orthologs. Only well conserved (>70%) amino acids are considered. Colours correspond to amino acid properties and match the multiple sequence alignment in Figure 1. **(C)** Codetta genetic code prediction. Log decoding probabilities for the UAA and UAG codons are shown for each of the 20 standard amino acids.

Figure 3: Example tRNA Genes. **(A)** Predicted secondary structure of an example tRNA-Sup(UUA) predicted to function as a lysine tRNA. The wobble position is highlighted. According to wobble-binding rules, uracil at this position can bind to either adenine or guanine in the third codon position of mRNA, allowing the suppressor tRNA to recognise both UAA and UAG stop codons. **(B)** Predicted secondary structure of an example tRNA-Sup(CUA) predicted to function as a glutamic acid tRNA. **(C)** Predicted secondary structure of the tRNA-SeC(UCA) for selenocysteine.

Figure 4: Enrichment of tandem stop codons. The proportion of codon positions occupied by UGA in the 20 in-frame codon positions immediately downstream of all genes and highly expressed genes. Positions where UGA is significantly overrepresented (chi-squared test, p-value < 0.05) are indicated with an asterisk.

Figure 5: **Phylogenomic analysis of genetic code changes in the Ciliophora.** Maximum-likelihood phylogeny of 46 ciliate species and 9 outgroup species from the Alveolata, based on a concatenated alignment of 89 BUSCO proteins (40,289 amino acid sites) under the LG+F+I+R7 model using IQ-TREE. The values at branches represent statistical support from 100 non-parametric bootstraps with the LG+F+I+R7 model, 100 non-parametric bootstraps from the IQ-TREE partitioned analysis, and Bayesian posterior probabilities determined under the CAT-GTR model in PhyloBayes-MPI. Branches with full support from all three approaches (i.e., 100/100/1) are indicated with solid black circles. Hyphens indicate branches that weren't recovered. Stop codon reassignments are shown (*, STOP; Q, glutamine; W, tryptophan; K, lysine; E, glutamic acid; Y, tyrosine; C, cysteine). The percentage of proteins included in the concatenated alignment is shown in the bar plot, highlighting the amount of missing data per species.

Supplementary Figure 1: Maximum-likelihood phylogeny of small subunit ribosomal RNA genes under the GTR+F+R5 model using IQ-TREE with 100 non-parametric bootstraps.

Supplementary Figure 2: Neighbour-Net phylogenetic network analysis of tRNA genes. tRNA genes predicted to be pseudogenes, contain introns, or that were excessively truncated were excluded. Lysine, glutamic acid, and suppressor tRNA genes are highlighted.

Supplementary Figure 3: Sequence frequency logo showing the nucleotide composition surrounding stop codons in all genes and in the subset of highly expressed genes.

Supplementary Figure 4: Bayesian phylogenomic analysis of 46 ciliate species and 9 outgroup Alveolata species, based on a concatenated alignment of 89 BUSCO proteins under the CAT-GTR model using PhyloBayes-MPI.

Supplementary Figure 5: Example multiple sequence alignments of *Plagiopyla frontata* genes with internal UGA codons identified by PhyloFisher with orthologous sequences spanning Eukaryota. **A)** TM9SF1. **B)** PIK3C3. **C)** CRNL1.

Table Captions

Table 1: Genome assembly and annotation statistics.

Supplementary Table 1: tRNA genes pairwise identities.

Supplementary Table 2: Datasets used for phylogenomics and genome annotation.

Supplementary Table 3: Amino acid and codon usage.

Table 1. Genome Assembly and Annotation Statistics

Genome Assembly	
Total length	69,715,444 bp
Contigs	3671
N50	59,570 bp
GC content	30.6%
RNA-Seq mapping rate	89%
BUSCO completeness[1]	Complete: 84.8% Complete and single copy: 80.1% Complete and duplicated: 4.7% Fragmented: 3.5% Missing: 11.7%
Genome Annotation	
Number of genes	20,141
Number of transcripts	22,084
Number of monoexonic genes	7,080
Exons per transcript	3.76
GC content (CDS)	34.12%
% of genome covered by CDS	63.8%
BUSCO completeness[1]	Complete: 94.74% Complete and single copy: 87.72% Complete and duplicated: 7.02% Fragmented: 1.75% Missing: 3.51%

	Median	**Mean**
CDS size (bp)	1,506	2,014.12
Intron size (bp)	57	80.39
5’UTR size (bp)	65	96.74
3’UTR size (bp)	95	137.61
Intergenic distances	156	574.43

[1] BUSCO completeness assessed using V4 with the Alveolata_obd10 dataset in genome mode for the genome assembly and in protein mode for the genome annotation.

References

1. Knight RD, Freeland SJ, Landweber LF. Rewiring the keyboard: evolvability of the genetic code. Nat Rev Genet. 2001;2: 49–58. doi:10.1038/35047500

2. Ivanova NN, Schwientek P, Tripp HJ, Rinke C, Pati A, Huntemann M, et al. Stop codon reassignments in the wild. Science. 2014;344: 909–913. doi:10.1126/science.1250691

3. Keeling PJ. Genomics: Evolution of the Genetic Code. Current Biology. 2016;26: R851–R853. doi:10.1016/j.cub.2016.08.005

4. Parfrey LW, Lahr DJG, Knoll AH, Katz LA. Estimating the timing of early eukaryotic diversification with multigene molecular clocks. Proceedings of the National Academy of Sciences. 2011;108: 13624–13629. doi:10.1073/pnas.1110633108

5. Prescott DM. The DNA of ciliated protozoa. 1994;58.

6. Arnaiz O, Mathy N, Baudry C, Malinsky S, Aury J-M, Denby Wilkes C, et al. The Paramecium Germline Genome Provides a Niche for Intragenic Parasitic DNA: Evolutionary Dynamics of Internal Eliminated Sequences. Malik HS, editor. PLoS Genet. 2012;8: e1002984. doi:10.1371/journal.pgen.1002984

7. Swart EC, Bracht JR, Magrini V, Minx P, Chen X, Zhou Y, et al. The Oxytricha trifallax Macronuclear Genome: A Complex Eukaryotic Genome with 16,000 Tiny Chromosomes. Eisen JA, editor. PLoS Biol. 2013;11: e1001473. doi:10.1371/journal.pbio.1001473

8. Lozupone CA, Knight RD, Landweber LF. The molecular basis of nuclear genetic code change in ciliates. Current Biology. 2001;11: 65–74. doi:10.1016/S0960-9822(01)00028-8

9. Heaphy SM, Mariotti M, Gladyshev VN, Atkins JF, Baranov PV. Novel Ciliate Genetic Code Variants Including the Reassignment of All Three Stop Codons to Sense Codons in *Condylostoma magnum*. Mol Biol Evol. 2016;33: 2885–2889. doi:10.1093/molbev/msw166

10. Meyer F, Schmidt HJ, Plümper E, Hasilik A, Mersmann G, Meyer HE, et al. UGA is translated as cysteine in pheromone 3 of Euplotes octocarinatus. Proc Natl Acad Sci USA. 1991;88: 3758–3761. doi:10.1073/pnas.88.9.3758

11. Swart EC, Serra V, Petroni G, Nowacki M. Genetic Codes with No Dedicated Stop Codon: Context-Dependent Translation Termination. Cell. 2016;166: 691–702. doi:10.1016/j.cell.2016.06.020

12. Slabodnick MM, Ruby JG, Reiff SB, Swart EC, Gosai S, Prabakaran S, et al. The Macronuclear Genome of Stentor coeruleus Reveals Tiny Introns in a Giant Cell. Current Biology. 2017;27: 569–575. doi:10.1016/j.cub.2016.12.057

13. Kryuchkova P, Grishin A, Eliseev B, Karyagina A, Frolova L, Alkalaeva E. Two-step model of stop codon recognition by eukaryotic release factor eRF1. Nucleic Acids Research. 2013;41: 4573–4586. doi:10.1093/nar/gkt113

14. Lekomtsev S, Kolosov P, Bidou L, Frolova L, Rousset J-P, Kisselev L. Different modes of stop codon restriction by the *Stylonychia* and *Paramecium* eRF1 translation termination factors. Proc Natl Acad Sci USA. 2007;104: 10824–10829. doi:10.1073/pnas.0703887104

15. Eliseev B, Kryuchkova P, Alkalaeva E, Frolova L. A single amino acid change of translation termination factor eRF1 switches between bipotent and omnipotent stop-codon specificity †. Nucleic Acids Research. 2011;39: 599–608. doi:10.1093/nar/gkq759

16. Hanyu N, Kuchino Y, Nishimura S, Beier H. Dramatic events in ciliate evolution: alteration of UAA and UAG termination codons to glutamine codons due to anticodon mutations in two *Tetrahymena* tRNAs $^{\mathrm{Gln}}$. The EMBO Journal. 1986;5: 1307–1311. doi:10.1002/j.1460-2075.1986.tb04360.x

17. Koonin EV, Novozhilov AS. Origin and evolution of the genetic code: The universal enigma. IUBMB Life. 2009;61: 99–111. doi:10.1002/iub.146

18. Liang H, Cavalcanti AR, Landweber LF. Conservation of tandem stop codons in yeasts. Genome Biol. 2005;6: R31. doi:10.1186/gb-2005-6-4-r31

19. Fleming I, Cavalcanti ARO. Selection for tandem stop codons in ciliate species with reassigned stop codons. Kapler GM, editor. PLoS ONE. 2019;14: e0225804. doi:10.1371/journal.pone.0225804

20. Adachi M, Cavalcanti ARO. Tandem Stop Codons in Ciliates That Reassign Stop Codons. J Mol Evol. 2009;68: 424–431. doi:10.1007/s00239-009-9220-y

21. Osawa S, Jukes TH, Watanabe K. Recent Evidence for Evolution of the Genetic Code. MICROBIOL REV. 1992;56.

22. Schultz DW, Yarus M. Transfer RNA Mutation and the Malleability of the Genetic Code. Journal of Molecular Biology. 1994;235: 1377–1380. doi:10.1006/jmbi.1994.1094

23. Andersson S, Kurland C. Genomic evolution drives the evolution of the translation system. Biochem Cell Biol. 1995;73: 775–787. doi:10.1139/o95-086

24. Mühlhausen S, Findeisen P, Plessmann U, Urlaub H, Kollmar M. A novel nuclear genetic code alteration in yeasts and the evolution of codon reassignment in eukaryotes. Genome Res. 2016;26: 945–955. doi:10.1101/gr.200931.115

25. Kollmar M, Mühlhausen S. Nuclear codon reassignments in the genomics era and mechanisms behind their evolution. BioEssays. 2017;39: 1600221. doi:10.1002/bies.201600221

26. Pánek T, Žihala D, Sokol M, Derelle R, Klimeš V, Hradilová M, et al. Nuclear genetic codes with a different meaning of the UAG and the UAA codon. BMC Biol. 2017;15: 8. doi:10.1186/s12915-017-0353-y

27. Crick FHC. Codon—anticodon pairing: The wobble hypothesis. Journal of Molecular Biology. 1996.

28. Macaulay IC, Haerty W, Kumar P, Li YI, Hu TX, Teng MJ, et al. G&T-seq: parallel sequencing of single-cell genomes and transcriptomes. Nat Methods. 2015;12: 519–522. doi:10.1038/nmeth.3370

29. Šlapeta J, Moreira D, López-García P. The extent of protist diversity: insights from molecular ecology of freshwater eukaryotes. Proc R Soc B. 2005;272: 2073–2081. doi:10.1098/rspb.2005.3195

30. Poláková K, Čepička I, Bourland WA. Phylogenetic Position of Three Well-known Ciliates from the Controversial Order Loxocephalida Jankowski, 1980 (Scuticociliatia, Oligohymenophorea) and Urozona buetschlii (Schewiakoff, 1889) with Improved Morphological Descriptions. Protist. 2021;172: 125833. doi:10.1016/j.protis.2021.125833

31. Gao F, Katz LA, Song W. Multigene-based analyses on evolutionary phylogeny of two controversial ciliate orders: Pleuronematida and Loxocephalida (Protista, Ciliophora, Oligohymenophorea). Molecular Phylogenetics and Evolution. 2013;68: 55–63. doi:10.1016/j.ympev.2013.03.018

32. Tice AK, Žihala D, Pánek T, Jones RE, Salomaki ED, Nenarokov S, et al. PhyloFisher: A phylogenomic package for resolving eukaryotic relationships. Hejnol A, editor. PLoS Biol. 2021;19: e3001365. doi:10.1371/journal.pbio.3001365

33. Shulgina Y, Eddy SR. A computational screen for alternative genetic codes in over 250,000 genomes. eLife. 2021;10: e71402. doi:10.7554/eLife.71402

34. Shulgina Y, Eddy SR. Codetta: predicting the genetic code from nucleotide sequence. Bioinformatics. 2023;39: btac802. doi:10.1093/bioinformatics/btac802

35. Chan PP, Lin BY, Mak AJ, Lowe TM. tRNAscan-SE 2.0: improved detection and functional classification of transfer RNA genes. Nucleic Acids Research. 2021;49: 9077–9096. doi:10.1093/nar/gkab688

36. Laslett D. ARAGORN, a program to detect tRNA genes and tmRNA genes in nucleotide sequences. Nucleic Acids Research. 2004;32: 11–16. doi:10.1093/nar/gkh152

37. Eisen JA, Coyne RS, Wu M, Wu D, Thiagarajan M, Wortman JR, et al. Macronuclear Genome Sequence of the Ciliate Tetrahymena thermophila, a Model Eukaryote. Gelfand M, editor. PLoS Biol. 2006;4: e286. doi:10.1371/journal.pbio.0040286

38. Krassowski T, Coughlan AY, Shen X-X, Zhou X, Kominek J, Opulente DA, et al. Evolutionary instability of CUG-Leu in the genetic code of budding yeasts. Nat Commun. 2018;9: 1887. doi:10.1038/s41467-018-04374-7

39. Mordret E, Dahan O, Asraf O, Rak R, Yehonadav A, Barnabas GD, et al. Systematic Detection of Amino Acid Substitutions in Proteomes Reveals Mechanistic Basis of Ribosome Errors and Selection for Translation Fidelity. Molecular Cell. 2019;75: 427-441.e5. doi:10.1016/j.molcel.2019.06.041

40. Aury J-M, Jaillon O, Duret L, Noel B, Jubin C, Porcel BM, et al. Global trends of whole-genome duplications revealed by the ciliate Paramecium tetraurelia. Nature. 2006;444: 171–178. doi:10.1038/nature05230

41. Salim HMW, Ring KL, Cavalcanti ARO. Patterns of Codon Usage in two Ciliates that Reassign the Genetic Code: Tetrahymena thermophila and Paramecium tetraurelia. Protist. 2008;159: 283–298. doi:10.1016/j.protis.2007.11.003

42. Dabrowski M, Bukowy-Bieryllo Z, Zietkiewicz E. Translational readthrough potential of natural termination codons in eucaryotes – The impact of RNA sequence. RNA Biology. 2015;12: 950–958. doi:10.1080/15476286.2015.1068497

43. Bonetti B, Fu L, Moon J, Bedwell DM. The Efficiency of Translation Termination is Determined by a Synergistic Interplay Between Upstream and Downstream Sequences inSaccharomyces cerevisiae. Journal of Molecular Biology. 1995;251: 334–345. doi:10.1006/jmbi.1995.0438

44. Beznosková P, Wagner S, Jansen ME, von der Haar T, Valášek LS. Translation initiation factor eIF3 promotes programmed stop codon readthrough. Nucleic Acids Research. 2015;43: 5099–5111. doi:10.1093/nar/gkv421

45. Poole ES, Brown CM, Tate WP. The identity of the base following the stop codon determines the efficiency of in vivo translational termination in Escherichia coli. EMBO J. 1995;14: 151–158.

46. Feng J-M, Jiang C-Q, Warren A, Tian M, Cheng J, Liu G-L, et al. Phylogenomic analyses reveal subclass Scuticociliatia as the sister group of subclass Hymenostomatia within class Oligohymenophorea. Molecular Phylogenetics and Evolution. 2015;90: 104–111. doi:10.1016/j.ympev.2015.05.007

47. Jiang C-Q, Wang G-Y, Xiong J, Yang W-T, Sun Z-Y, Feng J-M, et al. Insights into the origin and evolution of Peritrichia (Oligohymenophorea, Ciliophora) based on analyses of morphology and phylogenomics. Molecular Phylogenetics and Evolution. 2019;132: 25–35. doi:10.1016/j.ympev.2018.11.018

48. Gentekaki E, Kolisko M, Gong Y, Lynn D. Phylogenomics solves a long-standing evolutionary puzzle in the ciliate world: The subclass Peritrichia is monophyletic. Molecular Phylogenetics and Evolution. 2017;106: 1–5. doi:10.1016/j.ympev.2016.09.016

49. Wang C, Gao Y, Lu B, Chi Y, Zhang T, El-Serehy HA, et al. Large-scale phylogenomic analysis provides new insights into the phylogeny of the class Oligohymenophorea (Protista, Ciliophora) with establishment of a new subclass Urocentria nov. subcl. Molecular Phylogenetics and Evolution. 2021;159: 107112. doi:10.1016/j.ympev.2021.107112

50. Rotterová J, Salomaki E, Pánek T, Bourland W, Žihala D, Táborský P, et al. Genomics of New Ciliate Lineages Provides Insight into the Evolution of Obligate Anaerobiosis. Current Biology. 2020;30: 2037-2050.e6. doi:10.1016/j.cub.2020.03.064

51. Lasek-Nesselquist E, Johnson MD. A Phylogenomic Approach to Clarifying the Relationship of Mesodinium within the Ciliophora: A Case Study in the Complexity of Mixed-Species Transcriptome Analyses. Zufall R, editor. Genome Biology and Evolution. 2019;11: 3218–3232. doi:10.1093/gbe/evz233

52. Lynn DH, Kolisko M. Molecules illuminate morphology: phylogenomics confirms convergent evolution among 'oligotrichous' ciliates. International Journal of Systematic and Evolutionary Microbiology. 2017;67: 3676–3682. doi:10.1099/ijsem.0.002060

53. Chen X, Zhao X, Liu X, Warren A, Zhao F, Miao M. Phylogenomics of non-model ciliates based on transcriptomic analyses. Protein Cell. 2015;6: 373–385. doi:10.1007/s13238-015-0147-3

54. Seah BKB, Singh A, Swart EC. Karyorelict ciliates use an ambiguous genetic code with context-dependent stop/sense codons. Peer Community Journal. 2022;2. doi:10.24072/pcjournal.141

55. Bankevich A, Nurk S, Antipov D, Gurevich AA, Dvorkin M, Kulikov AS, et al. SPAdes: A New Genome Assembly Algorithm and Its Applications to Single-Cell Sequencing. Journal of Computational Biology. 2012;19: 455–477. doi:10.1089/cmb.2012.0021

56. Kang DD, Li F, Kirton E, Thomas A, Egan R, An H, et al. MetaBAT 2: an adaptive binning algorithm for robust and efficient genome reconstruction from metagenome assemblies. PeerJ. 2019;7: e7359. doi:10.7717/peerj.7359

57. von Meijenfeldt FAB, Arkhipova K, Cambuy DD, Coutinho FH, Dutilh BE. Robust taxonomic classification of uncharted microbial sequences and bins with CAT and BAT. Genome Biol. 2019;20: 217. doi:10.1186/s13059-019-1817-x

58. Karlicki M, Antonowicz S, Karnkowska A. Tiara: deep learning-based classification system for eukaryotic sequences. Birol I, editor. Bioinformatics. 2022;38: 344–350. doi:10.1093/bioinformatics/btab672

59. Gurevich A, Saveliev V, Vyahhi N, Tesler G. QUAST: quality assessment tool for genome assemblies. Bioinformatics. 2013;29: 1072–1075. doi:10.1093/bioinformatics/btt086

60. Manni M, Berkeley MR, Seppey M, Simão FA, Zdobnov EM. BUSCO Update: Novel and Streamlined Workflows along with Broader and Deeper Phylogenetic Coverage for

Scoring of Eukaryotic, Prokaryotic, and Viral Genomes. Kelley J, editor. Molecular Biology and Evolution. 2021;38: 4647–4654. doi:10.1093/molbev/msab199

61. Stanke M, Morgenstern B. AUGUSTUS: a web server for gene prediction in eukaryotes that allows user-defined constraints. Nucleic Acids Research. 2005;33: W465–W467. doi:10.1093/nar/gki458

62. Hubley R, Smit A. RepeatModeler. [cited 23 May 2022]. Available: https://www.repeatmasker.org/RepeatModeler/

63. Smit AF, Hubley R, Green P. RepeatMasker. [cited 23 May 2022]. Available: https://www.repeatmasker.org/

64. Kim D, Paggi JM, Park C, Bennett C, Salzberg SL. Graph-based genome alignment and genotyping with HISAT2 and HISAT-genotype. Nat Biotechnol. 2019;37: 907–915. doi:10.1038/s41587-019-0201-4

65. Mapleson D, Venturini L, Kaithakottil G, Swarbreck D. Efficient and accurate detection of splice junctions from RNA-seq with Portcullis. GigaScience. 2018;7: giy131. doi:10.1093/gigascience/giy131

66. Kovaka S, Zimin AV, Pertea GM, Razaghi R, Salzberg SL, Pertea M. Transcriptome assembly from long-read RNA-seq alignments with StringTie2. Genome Biology. 2019;20: 278. doi:10.1186/s13059-019-1910-1

67. Shao M, Kingsford C. Accurate assembly of transcripts through phase-preserving graph decomposition. Nat Biotechnol. 2017;35: 1167–1169. doi:10.1038/nbt.4020

68. Venturini L, Caim S, Kaithakottil GG, Mapleson DL, Swarbreck D. Leveraging multiple transcriptome assembly methods for improved gene structure annotation. GigaScience. 2018;7: giy093. doi:10.1093/gigascience/giy093

69. Bray NL, Pimentel H, Melsted P, Pachter L. Near-optimal probabilistic RNA-seq quantification. Nat Biotechnol. 2016;34: 525–527. doi:10.1038/nbt.3519

70. Katoh K, Standley DM. MAFFT Multiple Sequence Alignment Software Version 7: Improvements in Performance and Usability. Molecular Biology and Evolution. 2013;30: 772–780. doi:10.1093/molbev/mst010

71. Minh BQ, Schmidt HA, Chernomor O, Schrempf D, Woodhams MD, von Haeseler A, et al. IQ-TREE 2: New Models and Efficient Methods for Phylogenetic Inference in the Genomic Era. Teeling E, editor. Molecular Biology and Evolution. 2020;37: 1530–1534. doi:10.1093/molbev/msaa015

72. Kalyaanamoorthy S, Minh BQ, Wong TKF, von Haeseler A, Jermiin LS. ModelFinder: fast model selection for accurate phylogenetic estimates. Nat Methods. 2017;14: 587–589. doi:10.1038/nmeth.4285

73. Huson DH, Bryant D. Application of Phylogenetic Networks in Evolutionary Studies. Molecular Biology and Evolution. 2006;23: 254–267. doi:10.1093/molbev/msj030

74. Irwin NAT, Pittis AA, Mathur V, Howe LJ, Keeling PJ, Lynn DH, et al. The Function and Evolution of Motile DNA Replication Systems in Ciliates. Current Biology. 2021;31: 66-76.e6. doi:10.1016/j.cub.2020.09.077

75. Richter DJ, Berney C, Strassert JFH, Poh Y-P, Herman EK, Muñoz-Gómez SA, et al. EukProt: A database of genome-scale predicted proteins across the diversity of eukaryotes. Peer Community Journal. 2022;2. doi:10.24072/pcjournal.173

76. Grabherr MG, Haas BJ, Yassour M, Levin JZ, Thompson DA, Amit I, et al. Full-length transcriptome assembly from RNA-Seq data without a reference genome. Nat Biotechnol. 2011;29: 644–652. doi:10.1038/nbt.1883

77. Fu L, Niu B, Zhu Z, Wu S, Li W. CD-HIT: accelerated for clustering the next-generation sequencing data. Bioinformatics. 2012;28: 3150–3152. doi:10.1093/bioinformatics/bts565

78. Haas BJ, Papanicolaou A, Yassour M, Grabherr M, Blood PD, Bowden J, et al. De novo transcript sequence reconstruction from RNA-seq using the Trinity platform for reference generation and analysis. Nat Protoc. 2013;8: 1494–1512. doi:10.1038/nprot.2013.084

79. Capella-Gutierrez S, Silla-Martinez JM, Gabaldon T. trimAl: a tool for automated alignment trimming in large-scale phylogenetic analyses. Bioinformatics. 2009;25: 1972–1973. doi:10.1093/bioinformatics/btp348

80. Chernomor O, von Haeseler A, Minh BQ. Terrace Aware Data Structure for Phylogenomic Inference from Supermatrices. Syst Biol. 2016;65: 997–1008. doi:10.1093/sysbio/syw037

81. Lartillot N, Rodrigue N, Stubbs D, Richer J. PhyloBayes MPI: Phylogenetic Reconstruction with Infinite Mixtures of Profiles in a Parallel Environment. Systematic Biology. 2013;62: 611–615. doi:10.1093/sysbio/syt022

UAG
UAA
Oligohymenophorea sp. PL0344
Ichtyopthirius multifiliis
Tetrahymena thermophila
Paramecium tetraurelia
Stylonychia lemnae
Stentor coeruleus
Plasmodium falciparum
Oxyrrhis marina
Phytophthora parasitica
Thalassiosira pseudonana
Bigelowiella natans
Emiliania huxleyi
Guillardia theta
Chlamydomonas reinhardtii
Arabidopsis thaliana
Dictyostelium discoideum
Aspergillus fumigatus
Homo sapiens
Euglena gracilis
Naegleria gruberi
Giardia lamblia
Consensus
10
20
30
40
50
60
70
80
90
100
110
120
130
140
150
170
180
190
200
210
220
230
240
250
260
270
280
290
300
310
320
340
350
360
370
380
400
410
430

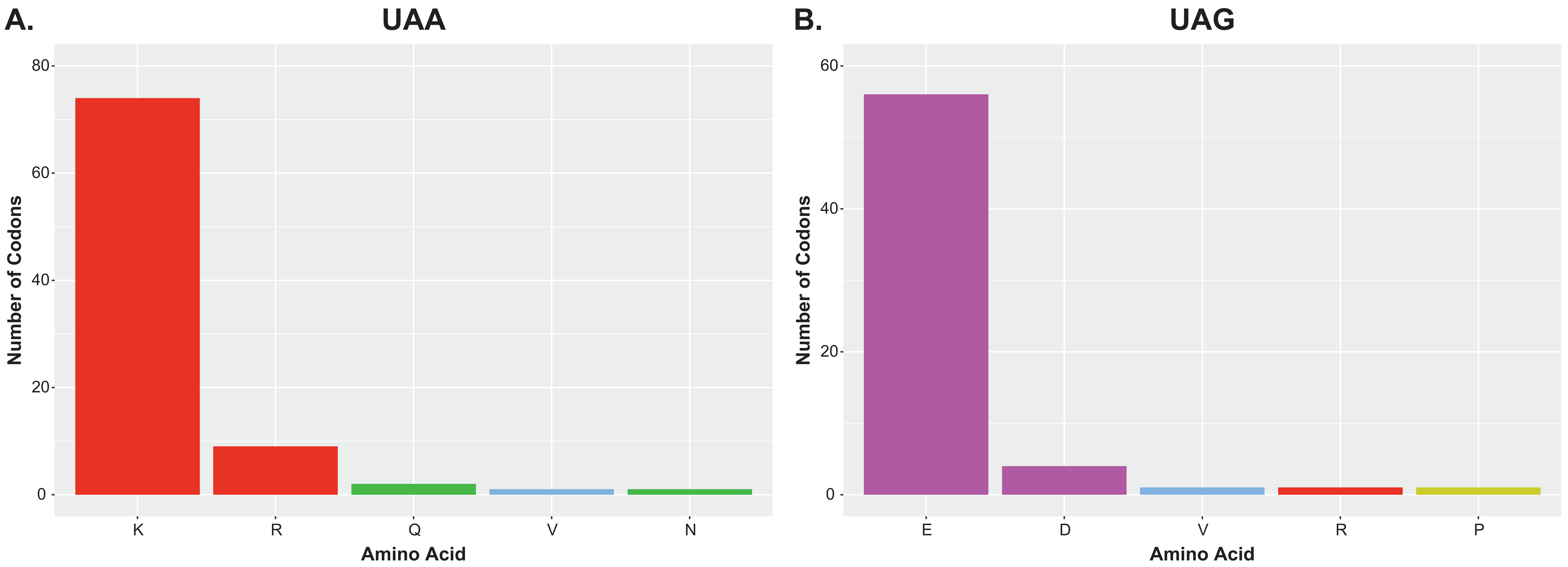

C.

Codetta Log Decoding Probabilities

	A	C	D	E	F	G	H	I	K	L	M	N	P	Q	R	S	T	V	W	Y	?
UAA	-7247.7	-12835.5	-8178.5	-5787.8	-14432.1	-10288.2	-6864.4	-12385.8	**0.0**	-10974.3	-10337.2	-6106.2	-11220.1	-4178.8	-3215.4	-6325.0	-6863.7	-10629.3	-15433.8	-11716.0	-3255.1
UAG	-5129.3	-9789.2	-3214.5	**0.0**	-10447.8	-7064.8	-5266.2	-9348.6	-4089.2	-8450.4	-8002.1	-4528.5	-7525.4	-3136.4	-4933.1	-4482.9	-5141.5	-8054.1	-11143.0	-8505.1	-2540.6

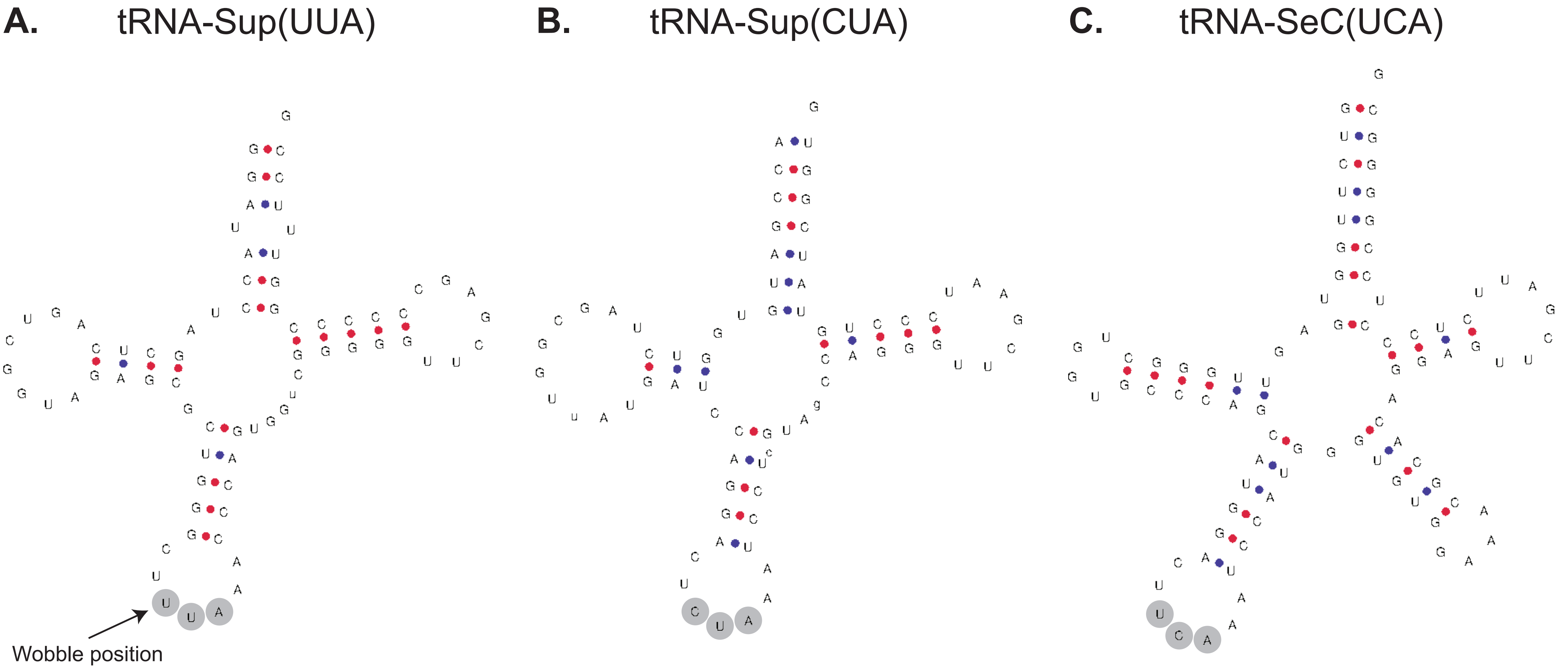
A.
tRNA-Sup(UUA)
B.
tRNA-Sup(CUA)
C.
tRNA-SeC(UCA)
U U A
C U A
U C A
Wobble position

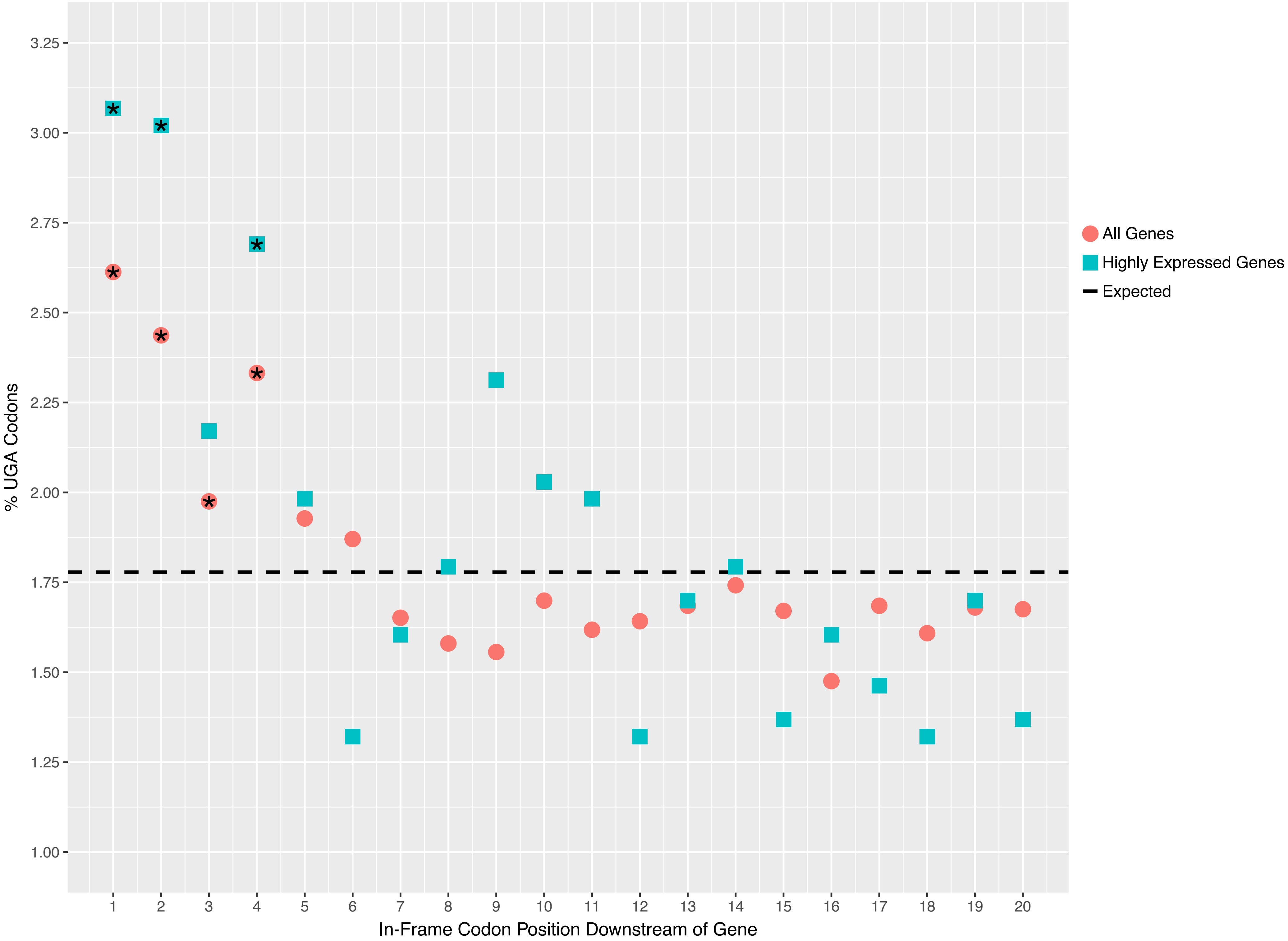
% UGA Codons
3.25
3.00
2.75
2.50
2.25
2.00
1.75
1.50
1.25
1.00
1
2
3
4
5
6
7
8
9
10
11
12
13
14
15
16
17
18
19
20
In-Frame Codon Position Downstream of Gene
All Genes
Highly Expressed Genes
Expected
*

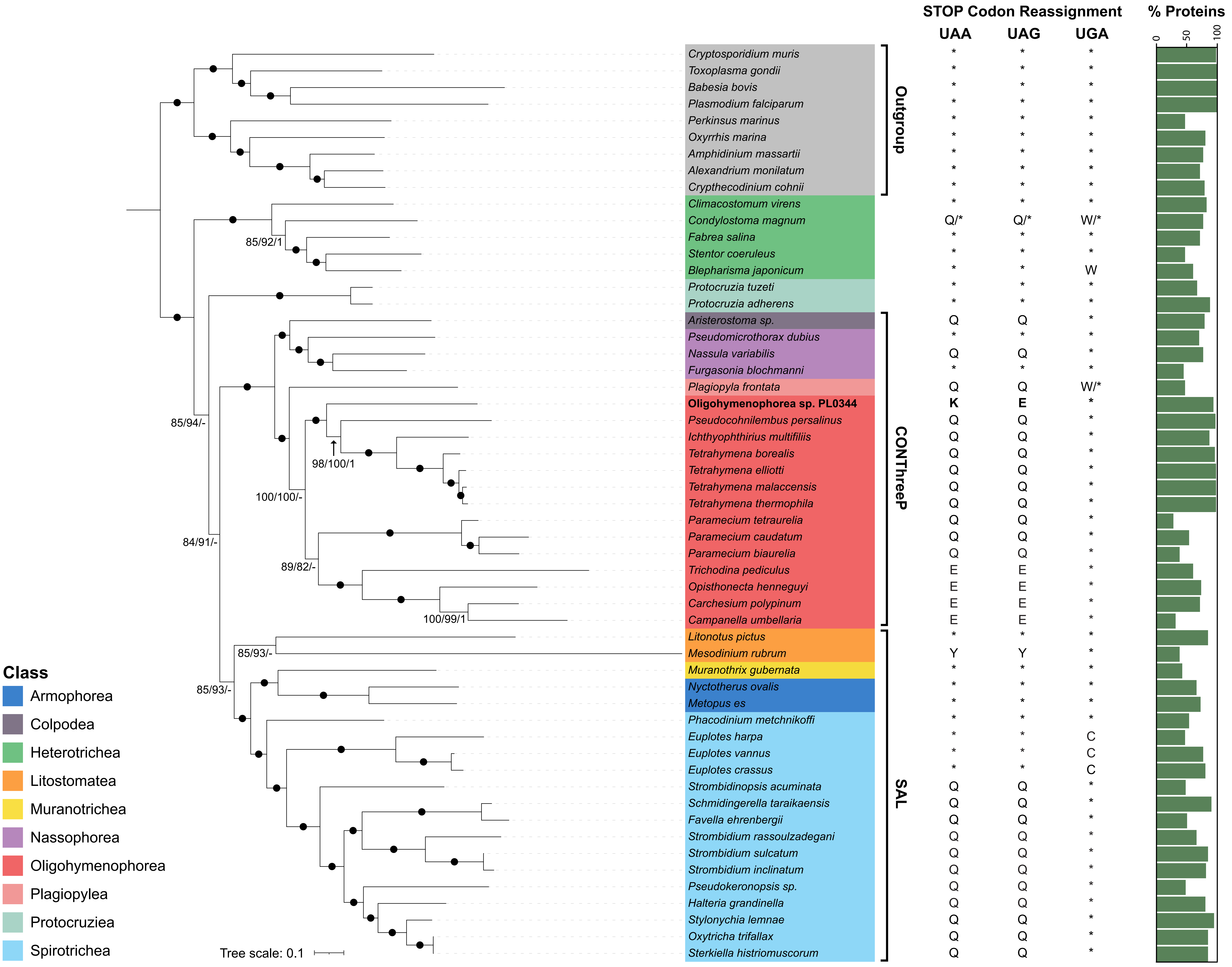
STOP Codon Reassignment
UAA
UAG
UGA
% Proteins
0
50
100
Cryptosporidium muris * * *
Toxoplasma gondii * * *
Babesia bovis * * *
Plasmodium falciparum * * *
Perkinsus marinus * * *
Oxyrrhis marina * * *
Amphidinium massartii * * *
Alexandrium monilatum * * *
Crypthecodinium cohnii * * *
Climacostomum virens * * *
Condylostoma magnum Q/* Q/* W/*
Fabrea salina * * *
Stentor coeruleus * * *
Blepharisma japonicum * * W
Protocruzia tuzeti * * *
Protocruzia adherens * * *
Aristerostoma sp. Q Q *
Pseudomicrothorax dubius * * *
Nassula variabilis Q Q *
Furgasonia blochmanni * * *
Plagiopyla frontata Q Q W/*
Oligohymenophorea sp. PL0344 **K** **E** *
Pseudocohnilembus persalinus Q Q *
Ichthyophthirius multifiliis Q Q *
Tetrahymena borealis Q Q *
Tetrahymena elliotti Q Q *
Tetrahymena malaccensis Q Q *
Tetrahymena thermophila Q Q *
Paramecium tetraurelia Q Q *
Paramecium caudatum Q Q *
Paramecium biaurelia Q Q *
Trichodina pediculus E E *
Opisthonecta henneguyi E E *
Carchesium polypinum E E *
Campanella umbellaria E E *
Litonotus pictus * * *
Mesodinium rubrum Y Y *
Muranothrix gubernata * * *
Nyctotherus ovalis * * *
Metopus es * * *
Phacodinium metchnikoffi * * *
Euplotes harpa * * C
Euplotes vannus * * C
Euplotes crassus * * C
Strombidinopsis acuminata Q Q *
Schmidingerella taraikaensis Q Q *
Favella ehrenbergii Q Q *
Strombidium rassoulzadegani Q Q *
Strombidium sulcatum Q Q *
Strombidium inclinatum Q Q *
Pseudokeronopsis sp. Q Q *
Halteria grandinella Q Q *
Stylonychia lemnae Q Q *
Oxytricha trifallax Q Q *
Sterkiella histriomuscorum Q Q *
Outgroup
CONThreeP
SAL
85/92/1
85/94/-
98/100/1
100/100/-
84/91/-
89/82/-
100/99/1
85/93/-
85/93/-
Tree scale: 0.1
Class
Armophorea
Colpodea
Heterotrichea
Litostomatea
Muranotrichea
Nassophorea
Oligohymenophorea
Plagiopylea
Protocruziea
Spirotrichea

Tree scale: 0.1
LC441007 1 Colpoda cucullus R2TTYS
EU264560 1 Colpodidium caudatum
MT253688 1 Nolandia nolandi strain CCAP 1613/15
KC832950 1 Plagiocampa sp PHB09022602
MW405099 1 Urozona buetschlii isolate UBBLUFF
AY102613 1 Paramecium tetraurelia
MT231343 1 Paramecium bursaria strain CCAP 1660 23
MW405094 1 Cinetochilum margaritaceum isolate CMAMP
AY821923 1 Uncultured oligohymenophorid ciliate clone CV1 2A 17
Oligohymenophorea sp. PL0344
HQ219368 1 Uncultured ciliate clone AY2009A9
LR025746 1 uncultured ciliate
HQ219418 1 Uncultured ciliate clone AY2009B17
AY212805 1 Dexiotrichides pangi
AF255357 1 Urocentrum turbo
EF114299 1 Urocentrum turbo clone 1
EF114300 1 Urocentrum turbo clone 2
AF401524 1 Campanella umbellaria
KJ690565 1 Ichthyophthirius multifiliis isolate G15/1-1702
KR778778 1 Tetrahymena rostrata clone TR1035
EF070245 1 Tetrahymena cosmopolitanis strain UM913
X56170 1 Tetrahymena canadensis
X56165 1 Tetrahymena thermophila
MK454743 1 Haptophrya planariarum clone RT42/10
MG819725 1 Dexiotricha colpidiopsis strain DEX201707a
JQ956542 1 Conchophthirus lamellidens strain FZ 1
JQ956543 1 Conchophthirus cucumis strain FZ 2
MN704274 1 Conchophthirus curtus isolate CC1
MN704275 1 Conchophthirus sp isolate CM1
LC466978 1 Scuticociliatia sp GW7 2
LC466984 1 Scuticociliatia sp GW7
JQ956551 1 Pseudocyclidium longum strain HN 7
FJ870103 1 Cinetochilum ovale isolate PHB08111304
FJ876969 1 Paratetrahymena parawassi isolate WYG061019
JX310019 1 Paratetrahymena wassi voucher JJM2009121511
EU744176 1 Paratetrahymena sp JJG
DQ103858 1 Uncultured marine eukaryote clone M3 18C08
EF527202 1 Uncultured marine eukaryote clone MA1 2D9
AY881632 1 Cardiostomatella vermiformis
MN437529 1 Platynematum rossellomorai isolate DEX201608
KF301567 1 Platynematum sp 1 TS 2013
FJ868188 1 Sathrophilus holtae isolate FXP2007102402
FJ868186 1 Sathrophilus planus isolate FXP2008103002 clone 1
JX310020 1 Pseudoplatynematum denticulatum voucher FXP2009042901
MW405098 1 Kariphilus muscorum isolate ZMCOTT
GQ330628 1 Uncultured Scuticociliatia clone PR2 3E 53
MW405097 1 Zitheron hovassei isolate ZHSMTUB
HQ446279 1 Metaradiophrya sp MCSK 2011
MN121076 1 Metaradiophrya varians isolate BZ 12 EF
MZ048835 1 Metaradiophrya chlorotica isolate JA 2 1M ACH
MN121071 1 Metaradiophrya lumbrici isolate KR 10/1 LT
HQ446282 1 Metaracoelophrya sp 2 MCSK 2011
MZ048824 1 Anoplophrya allolobophorae isolate JA 3 37 ACH
MZ048828 1 Anoplophrya octolasionis isolate MU 56 OL
MN121062 1 Anoplophrya lumbrici isolate RZ 6 LT
KF256816 1 Cristigera pleuronemoides isolate FXP2009091801
FJ868180 1 Cristigera media isolate FXP2008103001
GU479975 1 Uncultured Scuticociliatia clone PR3 4E 59
KF256822 1 Protocyclidium sinica isolate JJM2009113001
JQ956552 1 Protophyra ovicola strain HN 8
MT649635 1 Myxophyllum steenstrupi isolate KR 6 CL
KY886366 1 Cyclidium glaucoma isolate AP4
MN524102 1 Cyclidium vorax isolate PMM 20171026
KY476313 1 Cyclidium glaucoma
JQ692043 1 Uncultured Scuticociliatia clone 18S 23
KF256817 1 Cyclidium varibonneti isolate JJM2009121504
JQ956539 1 Ancistrum crassum strain HN 2
JQ956535 1 Ancistrum mytili strain HB 1
JQ956537 1 Ancistrum crassum strain HN 4
JQ956536 1 Ancistrum japonicum strain HN 5
KF256821 1 Protocyclidium citrullus isolate JJM2009120301
MF407350 1 Boveria labialis isolate ZZF20170501
HQ445965 1 Boveria subcylindricae
JX310022 1 Wilbertia typica voucher PXM20100628
JX310021 1 Eurystomatella sinica voucher PXM2010102701
U27816 1 Cyclidium plouneouri
FJ868185 1 Falcicyclidium fangi isolate LWW08033003
JX310012 1 Hippocomos salinus voucher FXP2009041402
FJ868182 1 Falcicyclidium atractodes isolate FXP08061106
JX310017 1 Pleuronema sp WS 2012 voucher PHB2009050101
EF486863 1 Pleuronema czapikae
JX310016 1 Pleuronema wiackowskii voucher XY2009113001
KT033423 1 Pleuronema parawiackowskii
JX310013 1 Histiobalantium minor voucher FXP2010042801
MT886454 1 Histiobalantium bodamicum isolate Leo2017050601
KU665372 1 Histiobalantium comosa
FJ156106 1 Schizocalyptra sinica isolate GD 1 WYG2007122002
EU744177 1 Schizocalyptra similis
EF486864 1 Pleuronema sinica
FJ848874 1 Pleuronema setigerum strain PHB08101402
KF840520 1 Pleuronema puytoraci isolate PXM2010122701
JX310018 1 Pleuronema coronatum voucher SZ2007033108
KU665357 1 Peniculistoma mytili isolate mussel 2 cell 4
JQ956546 1 Mytilophilus pacificae strain DL 4
KT033424 1 Pleuronema binucleatum
KF840519 1 Pleuronema grolierei isolate PXM2010050601
JX310015 1 Pleuronema setigerum voucher PXM2010042901
EU831192 1 Miamiensis avidus strain WD4
MH574792 1 Paramesanophrys typica
GQ214552 1 Glauconema trihymene strain PRA 270
U51554 1 Anophyroides haemophila
MT982807 1 Citrithrix smalli isolate LMJ2016091901
JQ956547 1 Myxophyllum magnum strain QD 3
EF527121 1 Uncultured marine eukaryote clone SA2 1D1
KJ760283 1 Uncultured eukaryote clone SGYS698
JN885085 1 Mesanophrys carcini isolate PXM2010022606
GU590870 1 Homalogastra setosa isolate JI 1
JQ956549 1 Paralembus digitiformis strain QD 4
MT982808 1 Homalogastra similis isolate QZS2017043001
MG581969 1 Homalogastra parasetosa isolate LMJ2016111302
EF527130 1 Uncultured marine eukaryote clone SA2 1G3
EF024585 1 Orchitophryidae environmental sample clone Elev 18S 904
EF158847 1 Homalogastra setosa isolate GT1 clone 18
AF527756 1 Schizocaryum dogieli
HM236335 1 Porpostoma notata isolate FXP2009050601
HM030719 1 Scuticociliatia sp Acropora/ciliate 2 2/CHN/2009
FJ648350 1 Philaster apodigitiformis
MG581968 1 Philasterides cf armatalis isolate LMJ2016040602
FJ848877 1 Philasterides armatalis strain GF2008062601
HM236339 1 Cohnilembus verminus isolate FXP2009051101
FJ858379 1 Paranophrys marina
AY314803 1 Metanophrys similis
AY835669 1 Pseudocohnilembus persalinus
FJ899594 1 Pseudocohnilembus longisetus
MT271860 1 Pseudocohnilembus sp isolate U 44
AY833087 1 Pseudocohnilembus hargisi
HM236338 1 Parauronema longum
AY541685 1 Plagiopyliella pacifica
AY541686 1 Thyrophylax vorax
AY541688 1 Entorhipidium tenue
AY541689 1 Entorhipidium pilatum
AY541690 1 Entorhipidium triangularis
MT271858 1 Biggaria sp isolate SK22 24
JQ956541 1 Biggaria bermudensis strain DL 3
JQ956548 1 Paranophrys magna strain KL 1
KY075872 1 Metanophrys sinensis isolate METSIN01
MT271859 1 Madsenia sp isolate SK22 23 26
JQ956550 1 Madsenia indomita strain HN 6
KU199245 1 Uronemita parabinucleata isolate LMJ2015080301
MH574793 1 Uronemella filificum
HM236337 1 Uronemella parafilificum isolate FXP2009053001
MK177640 1 Uncultured Uronema sp clone DDI259
JF973324 1 Uronema nigricans
MN524103 1 Apouronema harbinensis isolate PMM 20170506
MF072399 1 Uronema nigricans isolate LMJ2016120701
LN869943 1 Scuticociliatia sp aLPN3
FJ870100 Uronema heteromarinum
AY103190 Uronema elegans
MG581965 1 Uronema apomarinum isolate LMJ2016031201
DQ867074 1 Uronema marinum strain JK3
KC287215 1 Scuticociliatia SL 220
AY541687 1 Entodiscus borealis
FN598313 1 Uncultured Scuticociliatia
JN885087 1 Parauronema virginianum isolate PXM2010070302

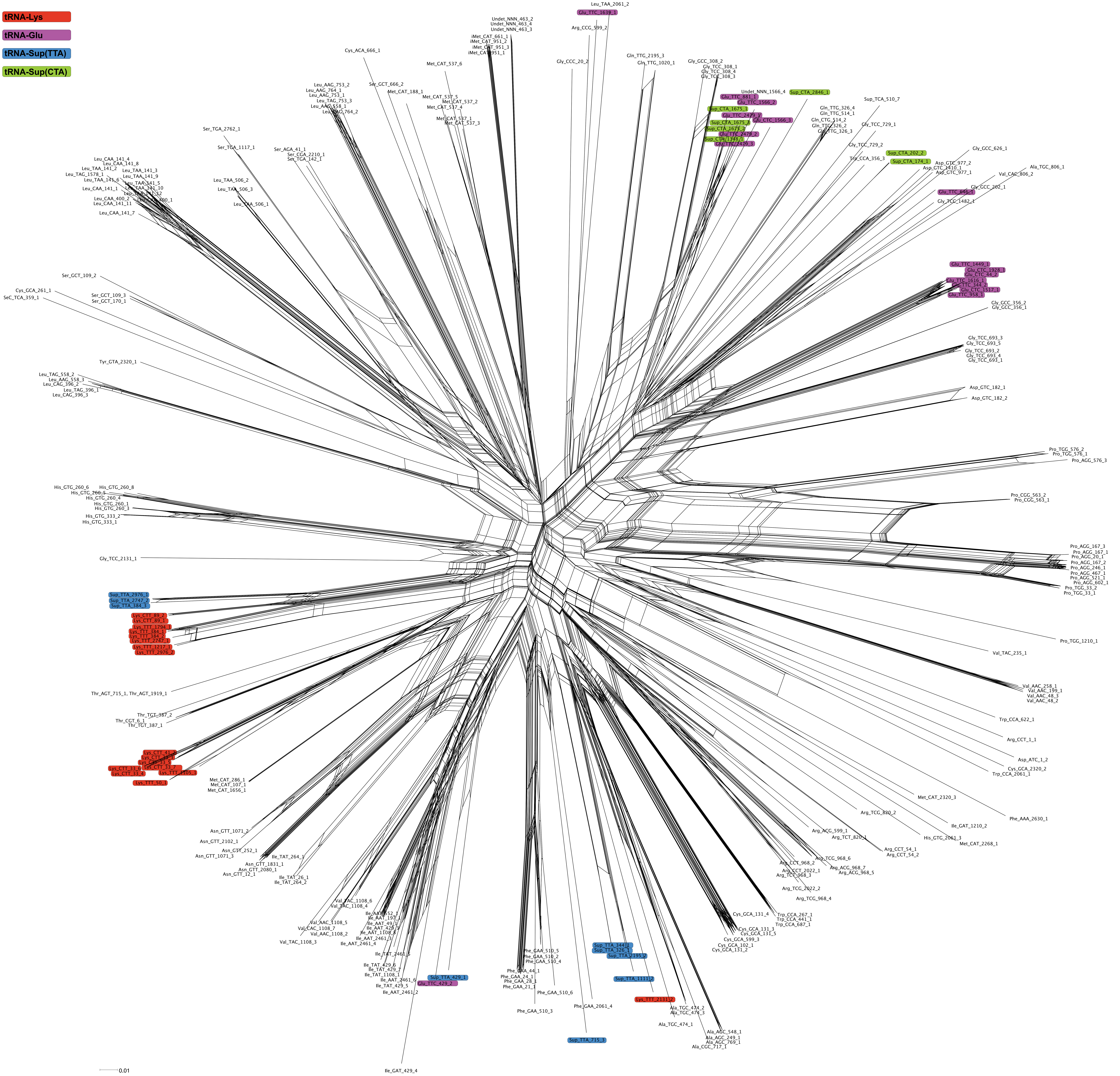
tRNA-Lys
tRNA-Glu
tRNA-Sup(TTA)
tRNA-Sup(CTA)
Leu_TAA_2061_2
Glu_TTC_1639_1
Arg_CCG_599_2
Undet_NNN_463_2
Undet_NNN_463_4
Undet_NNN_463_3
iMet_CAT_661_1
iMet_CAT_951_2
iMet_CAT_951_3
iMet_CAT_951_1
Cys_ACA_666_1
Met_CAT_537_6
Gly_CCC_20_2
Gln_TTG_2195_3
Gln_TTG_1020_1
Gly_GCC_308_2
Gly_TCC_308_1
Gly_TCC_308_4
Gly_TCC_308_3
Undet_NNN_1566_4
Sup_CTA_2846_1
Glu_TTC_881_1
Glu_TTC_1566_2
Sup_CTA_1675_1
Glu_TTC_2479_1
Glu_CTC_1566_3
Sup_CTA_1675_3
Sup_CTA_1675_2
Glu_TTC_2479_2
Sup_CTA_1348_1
Glu_TTC_2479_3
Sup_TCA_510_7
Gln_TTG_326_4
Gln_TTG_514_1
Gln_CTG_514_2
Gln_TTG_326_2
Gln_TTG_326_3
Gly_TCC_729_1
Gly_TCC_729_2
Sup_CTA_202_2
Trp_CCA_356_3
Sup_CTA_174_1
Gly_GCC_626_1
Asp_GTC_977_2
Asp_GTC_1410_1
Asp_GTC_977_1
Ala_TGC_806_1
Val_CAC_806_2
Gly_GCC_202_1
Glu_TTC_646_1
Gly_TCC_1482_1
Leu_AAG_753_2
Leu_AAG_764_1
Leu_AAG_753_1
Leu_TAG_753_3
Leu_AAG_558_1
Leu_CAG_764_2
Ser_GCT_666_2
Met_CAT_188_1
Met_CAT_537_5
Met_CAT_537_2
Met_CAT_537_4
Met_CAT_537_1
Met_CAT_537_3
Ser_TGA_2762_1
Ser_TGA_1117_1
Ser_AGA_41_1
Ser_CGA_2210_1
Ser_TGA_142_1
Leu_CAA_141_4
Leu_CAA_141_8
Leu_TAA_141_2
Leu_TAG_1578_1
Leu_TAA_141_6
Leu_CAA_141_1
Leu_CAA_400_2
Leu_CAA_141_11
Leu_CAA_141_7
Leu_TAA_141_3
Leu_TAA_141_9
Leu_TAA_141_5
Leu_TAA_141_10
Leu_TAA_141_12
Leu_CAA_400_1
Leu_TAA_506_2
Leu_TAA_506_3
Leu_TAA_506_1
Glu_TTC_1449_1
Glu_CTC_1928_1
Glu_CTC_44_2
Glu_TTC_1616_1
Glu_CTC_344_2
Glu_CTC_1517_1
Glu_TTC_958_1
Gly_GCC_356_2
Gly_GCC_356_1
Ser_GCT_109_2
Cys_GCA_261_1
SeC_TCA_359_1
Ser_GCT_109_3
Ser_GCT_170_1
Gly_TCC_693_3
Gly_TCC_693_5
Gly_TCC_693_2
Gly_TCC_693_4
Gly_TCC_693_1
Tyr_GTA_2320_1
Asp_GTC_182_1
Asp_GTC_182_2
Leu_TAG_558_2
Leu_AAG_558_3
Leu_CAG_396_2
Leu_TAG_396_1
Leu_CAG_396_3
Pro_TGG_576_2
Pro_TGG_576_1
Pro_AGG_576_3
His_GTG_260_6
His_GTG_260_8
His_GTG_260_5
His_GTG_260_4
His_GTG_260_1
His_GTG_260_3
His_GTG_333_2
His_GTG_333_1
Pro_CGG_563_2
Pro_CGG_563_1
Gly_TCC_2131_1
Pro_AGG_167_3
Pro_AGG_167_1
Pro_AGG_20_1
Pro_AGG_246_1
Pro_AGG_167_2
Pro_AGG_467_1
Pro_AGG_521_1
Pro_AGG_602_1
Pro_TGG_33_2
Pro_TGG_33_1
Sup_TTA_2976_1
Sup_TTA_2747_2
Sup_TTA_384_3
Lys_CTT_89_2
Lys_CTT_89_1
Lys_TTT_1794_1
Lys_TTT_384_1
Lys_TTT_384_2
Lys_TTT_2747_1
Lys_TTT_1217_1
Lys_TTT_2976_2
Pro_TGG_1210_1
Val_TAC_235_1
Thr_AGT_715_1, Thr_AGT_1919_1
Val_AAC_258_1
Val_AAC_199_1
Val_AAC_48_3
Val_AAC_48_2
Thr_TGT_387_2
Thr_CGT_6_1
Thr_TGT_387_1
Trp_CCA_622_1
Arg_CCT_1_1
Lys_CTT_41_2
Lys_CTT_33_1
Lys_CTT_33_5
Lys_CTT_33_6
Lys_CTT_33_7
Lys_CTT_33_4
Lys_TTT_1105_1
Lys_TTT_50_1
Met_CAT_286_1
Met_CAT_107_1
Met_CAT_1656_1
Asp_ATC_1_2
Cys_GCA_2320_2
Trp_CCA_2061_1
Met_CAT_2320_3
Phe_AAA_2630_1
Arg_TCG_820_2
Ile_GAT_1210_2
Arg_ACG_599_1
Arg_TCT_820_1
His_GTG_2061_3
Met_CAT_2268_1
Asn_GTT_1071_2
Asn_GTT_2102_1
Asn_GTT_252_1
Asn_GTT_1071_3
Ile_TAT_264_1
Asn_GTT_1831_1
Asn_GTT_2080_1
Asn_GTT_12_1
Ile_TAT_26_1
Ile_TAT_264_2
Arg_TCG_968_6
Arg_CCT_968_2
Arg_ACG_968_7
Arg_CCT_2022_1
Arg_ACG_968_5
Arg_TCT_968_3
Arg_CCT_54_1
Arg_CCT_54_2
Arg_TCG_2022_2
Arg_TCG_968_4
Val_TAC_1108_6
Val_TAC_1108_4
Val_AAC_1108_5
Val_CAC_1108_7
Val_AAC_1108_2
Val_TAC_1108_3
Ile_AAT_552_1
Ile_AAT_197_1
Ile_AAT_49_1
Ile_AAT_429_3
Ile_AAT_1108_8
Ile_AAT_2461_3
Ile_AAT_2461_4
Ile_TAT_2461_5
Ile_TAT_429_6
Ile_TAT_429_7
Ile_TAT_1108_1
Ile_AAT_2461_6
Ile_TAT_429_5
Ile_AAT_2461_2
Sup_TTA_429_1
Glu_TTC_429_2
Cys_GCA_131_4
Trp_CCA_267_1
Trp_CCA_441_1
Trp_CCA_687_1
Cys_GCA_131_3
Cys_GCA_131_5
Cys_GCA_599_3
Cys_GCA_102_1
Cys_GCA_131_2
Phe_GAA_510_5
Phe_GAA_510_2
Phe_GAA_510_4
Phe_GAA_44_1
Phe_GAA_24_1
Phe_GAA_28_1
Phe_GAA_21_1
Phe_GAA_510_6
Phe_GAA_510_3
Phe_GAA_2061_4
Sup_TTA_344_1
Sup_TTA_326_1
Sup_TTA_2195_2
Sup_TTA_1111_2
Lys_TTT_2131_2
Ala_TGC_474_2
Ala_TGC_474_3
Ala_TGC_474_1
Ala_AGC_548_1
Ala_AGC_249_1
Ala_AGC_769_1
Ala_CGC_717_1
Sup_TTA_715_3
Ile_GAT_429_4
0.01

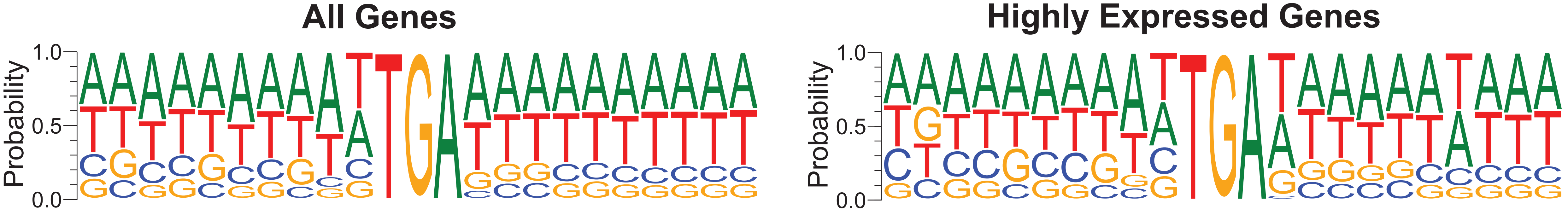
All Genes

Highly Expressed Genes

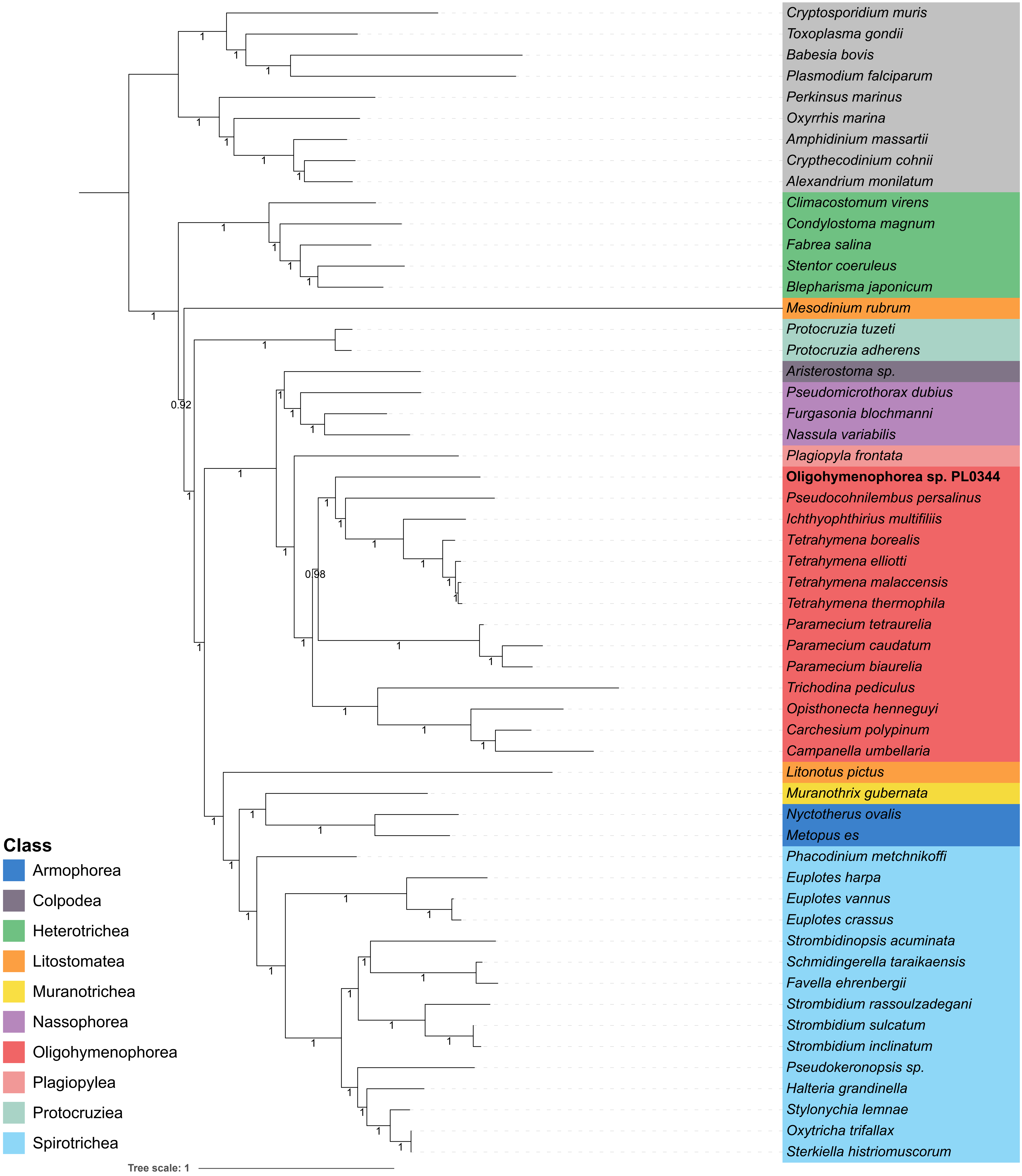
Cryptosporidium muris
Toxoplasma gondii
Babesia bovis
Plasmodium falciparum
Perkinsus marinus
Oxyrrhis marina
Amphidinium massartii
Crypthecodinium cohnii
Alexandrium monilatum
Climacostomum virens
Condylostoma magnum
Fabrea salina
Stentor coeruleus
Blepharisma japonicum
Mesodinium rubrum
Protocruzia tuzeti
Protocruzia adherens
Aristerostoma sp.
Pseudomicrothorax dubius
Furgasonia blochmanni
Nassula variabilis
Plagiopyla frontata
Oligohymenophorea sp. PL0344
Pseudocohnilembus persalinus
Ichthyophthirius multifiliis
Tetrahymena borealis
Tetrahymena elliotti
Tetrahymena malaccensis
Tetrahymena thermophila
Paramecium tetraurelia
Paramecium caudatum
Paramecium biaurelia
Trichodina pediculus
Opisthonecta henneguyi
Carchesium polypinum
Campanella umbellaria
Litonotus pictus
Muranothrix gubernata
Nyctotherus ovalis
Metopus es
Phacodinium metchnikoffi
Euplotes harpa
Euplotes vannus
Euplotes crassus
Strombidinopsis acuminata
Schmidingerella taraikaensis
Favella ehrenbergii
Strombidium rassoulzadegani
Strombidium sulcatum
Strombidium inclinatum
Pseudokeronopsis sp.
Halteria grandinella
Stylonychia lemnae
Oxytricha trifallax
Sterkiella histriomuscorum
0.92
0.98
1
Class
Armophorea
Colpodea
Heterotrichea
Litostomatea
Muranotrichea
Nassophorea
Oligohymenophorea
Plagiopylea
Protocruziea
Spirotrichea
Tree scale: 1

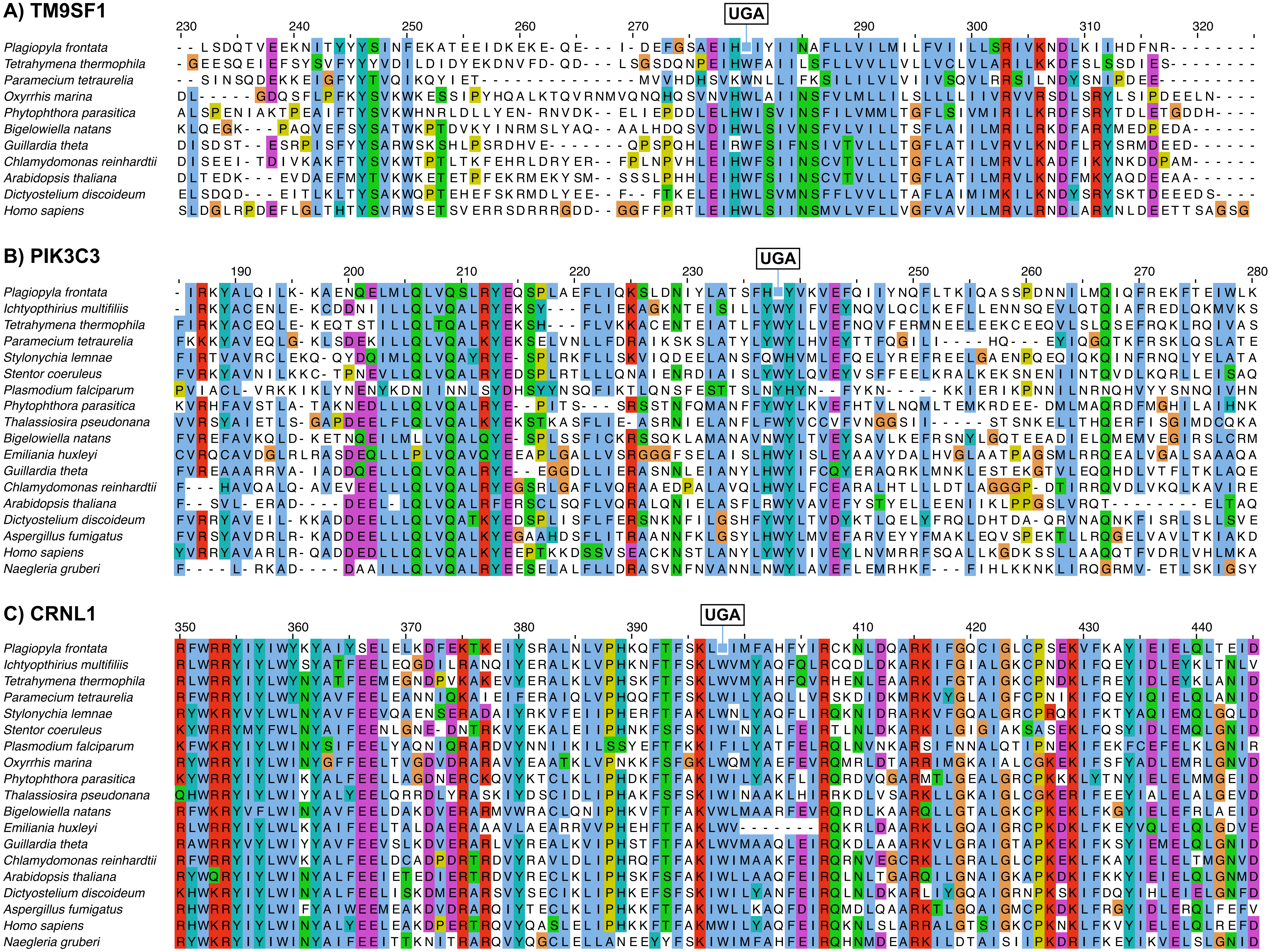

A) TM9SF1

```
Plagiopyla frontata        --LSDQTVEEKNITYYYSINFEKATEEIDKEKE-QE---I-DEFGSAEIH IYIINAFLLVILMILFVIILLSRIVKNDLKIIHDFNR-------
Tetrahymena thermophila    -GEESQEIEFSYSVFYYYVDILDIDYEKDNVFD-QD---LSGSDQNPEIHWFAIILSFLLVVLLVLLVCLVLARILKKDFSLSSDIES-------
Paramecium tetraurelia     --SINSQDEKKEIGFYYTVQIKQYIET--------------MVVHDHSVKWNLLIFKSILILVLVIIVSQVLRRSILNDYSNIPDEE--------
Oxyrrhis marina            DL-----GDQSFLPFKYSVKWKESSIPYHQALKTQVRNMVQNQHQSVNVHWLAIINSFVLMLLILSLLLLIIVRVVRSDLSRYLSIPDEELN---
Phytophthora parasitica    ALSPENIAKTPEAIFTYSVKWHNRLDLLYEN-RNVDK--ELIEPDDLELHWISVINSFILVMMLTGFLSIVMIRILKRDFSRYTDLETGDDH---
Bigelowiella natans        KLQEGK---PAQVEFSYSATWKPTDVKYINRMSLYAQ--AALHDQSVDIHWLSIVNSFVLVILLTSFLAIILMRILRKDFARYMEDPEDA-----
Guillardia theta           DISDST--ESRPISFYYSARWSKSHLPSRDHVE-------QPSPQHLEIRWFSIFNSIVTVLLLTGFLATILVRVLKNDFLRYSRMDEED-----
Chlamydomonas reinhardtii  DISEEI-TDIVKAKFTYSVKWTPTLTKFEHRLDRYER--FPLNPVHLEIHWFSIINSCVTVLLLTGFLATILMRVLKADFIKYNKDDPAM-----
Arabidopsis thaliana       DLTEDK---EVDAEFMYTVKWKETETPFEKRMEKYSM--SSSLPHHLEIHWFSIINSCVTVLLLTGFLATILMRVLKNDFMKYAQDEEAA-----
Dictyostelium discoideum   ELSDQD---EITLKLTYSAKWQPTEHEFSKRMDLYEE--F--FTKELEIHWLSVMNSFFLVVLLTAFLAIMIMKILKNDYSRYSKTDEEEDS---
Homo sapiens               SLDGLRPDEFLGLTHTYSVRWSETSVERRSDRRRGDD--GGFFPRTLEIHWLSIINSMVLVFLLVGFVAVILMRVLRNDLARYNLDEETTSAGSG
```

B) PIK3C3

```
Plagiopyla frontata        -IRKYALQILK-KAENQELMLQLVQSLRYEQSPLAEFLIQKSLDNIYLATSFH YVKVEFQIIYNQFLTKIQASSPDNNILMQIQFREKFTEIWLK
Ichtyopthirius multifiliis -IRKYACENLE-KCDDNIILLQLVQALRYEKSY---FLIEKAGKNTEISILLYWYIFVEYNQVLQCLKEFLLENNSQEVLQTQIAFREDLQKMVKS
Tetrahymena thermophila    FIRKYACEQLE-KEQTSTILLQLTQALRYEKSH---FLVKKACENTEIATLFYWYLLVEFNQVFERMNEELEEKCEEQVLSLQSEFRQKLRQIVAS
Paramecium tetraurelia     FKKKYAVEQLG-KLSDEKILLQLVQALKYEKSELVNLLFDRAIKSKSLATYLYWYLHVEYTTFQGILI----HQ---EYIQGQTKFRSKLQSLATE
Stylonychia lemnae         FIRTVAVRCLEKQ-QYDQIMLQLVQAYRYE-SPLRKFLLSKVIQDEELANSFQWHVMLEFQELYREFREELGAENPQEQIQKQINFRNQLYELATA
Stentor coeruleus          FVRKYAVNILKKC-TPNEVLLQLVQALRYEDSPLRTLLLQNAIENRDIAISLYWYLQVEYVSFFEELKRALKEKSNENIINTQVDLKQRLLEISAQ
Plasmodium falciparum      PVIACL-VRKKIKLYNENYKDNIINNLSYDHSYYNSQFIKTLQNSFESTTSLNYHYN--FYKN-----KKIERIKPNNILNRNQHVYYSNNQIVHN
Phytophthora parasitica    KVRHFAVSTLA-TAKNEDLLLQLVQALRYE--PITS---SRSSTNFQMANFFYWYLKVEFHTVLNQMLTEMKRDEE-DMLMAQRDFMGHILAIHNK
Thalassiosira pseudonana   VVRSYAIETLS-GAPDEELFLQLVQALKYEKSTKASFLIE-ASRNIELANFLFWYVCCVFVNGGSII-----STSNKELLTHQERFISGIMDCQKA
Bigelowiella natans        FVREFAVKQLD-KETNQEILMLLVQALQYE-SPLSSFICKRSSQKLAMANAVNWYLTVEYSAVLKEFRSNYLGQTEEADIELQMEMVEGIRSLCRM
Emiliania huxleyi          CVRQCAVDGLRLRASDEQLLLPLVQAVQYEEAPLGALLVSRGGGFSELAISLHWYISLEYAAVYDALHVGLAATPAGSMLRRQEALVGALSAAAQA
Guillardia theta           FVREAAARRVA-IADDQELLLQLVQALRYE--EGGDLLIERASNNLEIANYLHWYIFCQYERAQRKLMNKLESTEKGTVLEQQHDLVTFLTKLAQE
Chlamydomonas reinhardtii  F---HAVQALQ-AVEVEELLLQLVQALRYEGSRLGAFLVQRAAEDPALAVQLHWYLFCEARALHTLLLDTLAGGGP-DTIRRQVDLVKQLKAVIRE
Arabidopsis thaliana       F--SVL-ERAD----DEEL-LQLVQALRFERSCLSQFLVQRALQNIELASFLRWYVAVEFYSTYELLEENIIKLPPGSLVRQT--------ELTAQ
Dictyostelium discoideum   FVRRYAVEIL-KKADDEELLLQLVQATKYEDSPLISFLFERSNKNFILGSHFYWYLTVDYKTLQELYFRQLDHTDA-QRVNAQNKFISRLSLLSVE
Aspergillus fumigatus      FVRSYAVDRLR-KADDEELLLQLVQALKYEGAAHDSFLITRAANNFKLGSYLHWYLMVEFARVEYYFMAKLEQVSPEKTLLRQGELVAVLTKIAKD
Homo sapiens               YVRRYAVARLR-QADDEDLLLQLVQALKYEEPTKKDSSVSEACKNSTLANYLYWYVIVEYLNVMRRFSQALLKGDKSSLLAAQQTFVDRLVHLMKA
Naegleria gruberi          F----L-RKAD----DAAILLQLVQALRYEESELALFLLDRASVNFNVANNLNWYLAVEFLEMRHKF---FIHLKKNKLIRQGRMV-ETLSKIGSY
```

C) CRNL1

```
Plagiopyla frontata        RFWRRYIYIWYKYAIYSELELKDFEKTKEIYSRALNLVPHKQFTFSKL IMFAHFYIRCKNLDQARKIFGQCIGLCPSEKVFKAYIEIELQLTEID
Ichtyopthirius multifiliis RLWRRYIYLWYSYATFEELEQGDILRANQIYERALKLVPHKNFTFSKLWVMYAQFQLRCQDLDKARKIFGIALGKCPNDKIFQEYIDLEYKLTNLV
Tetrahymena thermophila    RLWRRYIYLWYNYATFEEMEGNDPVKAKEVYERALKLVPHSKFTFSKLWVMYAHFQVRHENLEAARKIFGTAIGKCPNDKLFREYIDLEYKLANID
Paramecium tetraurelia     RFWRRYIYLWYNYAVFEELEANNIQKAIEIFERAIQLVPHQQFTFSKLWILYAQLLVRSKDIDKMRKVYGLAIGFCPNIKIFQEYIQIELQLANID
Stylonychia lemnae         RYWKRYVYLWLNYAVFEEVQAENSERADAIYRKVFEIIPHERFTFAKLWNLYAQFLIRQKNIDRARKVFGQALGRCPRQKIFKTYAQIEMQLGQLD
Stentor coeruleus          KYWRRYMYFWLNYAIFEENLGNE-DNTRKVYEKALEIIPHNKFSFSKIWINYALFEIRTLNLDKARKILGIGIAKSASEKLFQSYIDLEMQLGNID
Plasmodium falciparum      KFWKRYIYLWINYSIFEELYAQNIQRARDVYNNIIKILSSYEFTFKKIFILYATFELRQLNVNKARSIFNNALQTIPNEKIFEKFCEFELKLGNIR
Oxyrrhis marina            RYWRRYIYLWINYGFFEELTVGDVDRARAVYEAATKLVPNKKFSFGKLWQMYAEFEVRQMRLDTARRIMGKAIALCGKEKIFSFYADLEMRLGNVD
Phytophthora parasitica    KYWRRYIYLWIKYALFEELLAGDNERCKQVYKTCLKLIPHDKFTFAKIWILYAKFLIRQRDVQGARMTLGEALGRCPKKKLYTNYIELELMMGEID
Thalassiosira pseudonana   QHWRRYIYLWIYYALYEELQRRDLYRASKIYDSCIDLIPHAKFSFSKIWINAAKLHIRRKDLVSARKLLGKAIGLCGKERIFEEYIALELALGEVD
Bigelowiella natans        RFWKRYVFLWINYAVFEELDAKDVERARMVWRACLQNIPHKVFTFAKVWLMAARFEVRQRDLKAARQLLGTALGKCPKEKLFKGYIELEFRLAEID
Emiliania huxleyi          RLWRRYIYLWLKYAIFEELTALDAERAAAVLAEARRVVPHEHFTFAKLWV-------RQKRLDAARKLLGQAIGRCPKDKLFKEYVQLELQLGDVE
Guillardia theta           RAWRRYVYLWIYYAVFEEVSLKDVERARLVYREALKVIPHSTFTFAKLWVMAAQLEIRQKDLAAARKVLGRAIGTAPKEKIFKSYIEMELQLGNID
Chlamydomonas reinhardtii  RFWRRYIYLWVKYALFEELDCADPDRTRDVYRAVLDLIPHRQFTFAKIWIMAAKFEIRQRNVEGCRKLLGRALGLCPKEKLFKAYIELELTMGNVD
Arabidopsis thaliana       RYWQRYIYLWINYALFEEIETEDIERTRDVYRECLKLIPHSKFSFAKIWLLAAQFEIRQLNLTGARQILGNAIGKAPKDKIFKKYIEIELQLGNMD
Dictyostelium discoideum   KHWKRYIYLWINYALFEELISKDMERARSVYSECIKLIPHKEFSFSKIWILYANFEIRQLNLDKARLIYGQAIGRNPKSKIFDQYIHLEIELGNFD
Aspergillus fumigatus      RHWRRYIYLWIFYAIWEEMEAKDVDRARQIYTECLKLIPHKKFTFAKIWLLKAQFDIRQMDLQAARKTLGQAIGMCPKDKLFRGYIDLERQLFEFV
Homo sapiens               RHWKRYIYLWINYALYEELEAKDPERTRQVYQASLELIPHKKFTFAKMWILYAQFEIRQKNLSLARRALGTSIGKCPKNKLFKVYIELELQLREFD
Naegleria gruberi          RYWKRYIYIWINYAIFEEITTKNITRARQVYQGCLELLANEEYYFSKIWIMFAHFEIRQHNMDEARKILDTAISIIPKDRIFKEYIKVELSLGNID
```